INSIGHTS INTO THE ROLE OF HYDF-CATALYZED GTP ACTIVITY IN HYDROGENASE MATURATION

by

Alexandra Lee Bueling

A thesis submitted in partial fulfillment
of the requirements for the degree

of

Master of Science

in

Biochemistry

MONTANA STATE UNIVERSITY
Bozeman, Montana

July 2009

©COPYRIGHT

by

Alexandra Lee Bueling

2009

All Rights Reserved

APPROVAL

of a thesis submitted by

Alexandra Lee Bueling

This thesis has been read by each member of the thesis committee and has been found to be satisfactory regarding content, English usage, format, citation, bibliographic style, and consistency, and is ready for submission to the Division of Graduate Education.

Dr. Joan Broderick

Approved for the Department of Chemistry and Biochemistry

Dr. David Singel

Approved for the Division of Graduate Education

Dr. Carl A. Fox

STATEMENT OF PERMISSION TO USE

In presenting this thesis in partial fulfillment of the requirements for a master's degree at Montana State University, I agree that the Library shall make it available to borrowers under rules of the Library.

If I have indicated my intention to copyright this thesis by including a copyright notice page, copying is allowable only for scholarly purposes, consistent with "fair use" as prescribed in the U.S. Copyright Law. Requests for permission for extended quotation from or reproduction of this thesis in whole or in parts may be granted only by the copyright holder.

Alexandra Lee Bueling

July 2009

ACKNOWLEDGEMENTS

Many thanks to my advisor Dr. Joan Broderick who was of immense help during this project, and Dr. Eric Shepard for his guidance. Also, thank you to Eric Bueling for assistance in editing, formatting, and keeping things running smoothly.

TABLE OF CONTENTS

1. INTRODUCTION....1

Iron Sulfur Clusters....2
[NiFe]-Hydrogenase....3
[FeFe]-Hydrogenase....5
Hydrogenase Accessory Proteins....8
Radical SAM Enzymes HydE and HydG....8
HydF....11

2. MATERIALS AND METHODS....13

Cell Growth....13
Protein Purification....13
Iron-Depleted and Reconstituted HydF....15
Quantifying Protein and Iron Content....16
GTPase Assays and HPLC Analysis....17

3. DATA AND RESULTS....19

Protein Purification and Characterization....19
HydF....19
HydG....21
HydE....22
HydF Glycine to Alanine Mutations....23
HydF Serine to Alanine Mutations....25
HydF Cysteine to Serine Mutations....27
Generation of Iron-Depleted and Reconstituted HydF....27
GTPase Assays....28
Effects of Cluster Content....30
Effects of Accessory and Structural Hyd Proteins....31
Role of Specific HydF Residues....34

4. DISCUSSION....39

Effects of Metal Cluster Content....39
Effect of Other Hyd Proteins on GTPase Activity....39
Role of Specific HydF Residues in GTP Hydrolysis....40

5. CONCLUSION....45

REFERENCES CITED....47

LIST OF TABLES

Table Page

1. Catalytic Activity for $HydF^{EG}$ in the presence of Structural and Accessory Protein.....32

2. Catalytic Activity for HydF Mutations.....38

LIST OF FIGURES

Figure Page

1.1 Active site and structure of the [NiFe] hydrogenase.....4

1.2 Crystal structures of CpI, (PDB ID 1FEH)(1.8 Å) and DdH (PDB ID 1HFE)(1.6 Å) 5

1.3 Active site of the *C. pasteurianum* [Fe-Fe] Hydrogenase.....6

3.1 SDS-PAGE analysis of fractions from a $HydF^{\Delta EG}$ purification.....19

3.2 Purification of $HydF^{EG}$.....20

3.3 SDS-PAGE analysis of fractions from a $HydG^{\Delta EF}$ purification.....21

3.4 SDS-PAGE analysis of fractions from a $HydG^{EF}$ purification.....22

3.5 SDS-PAGE analysis of fractions from a $HydE^{FG}$ purification.....23

3.6 Purification of $HydF(G19A)^{\Delta EG}$.....24

3.7 SDS-PAGE analysis of a $HydF(G24A)^{\Delta EG}$ mutant purification.....25

3.8 SDS-PAGE analysis of a $HydF(S26A)^{\Delta EG}$ mutant purification.....26

3.9 SDS-PAGE analysis of a $HydF(S26A)^{EG}$ mutant purification.....26

3.10 SDS-PAGE analysis of a $HydF^{\Delta EG}$ C353S mutant purification.....27

3.11 UV-visible spectra of $HydF^{\Delta EG}$ stripped of metal and $HydF^{\Delta EG}$ with reconstituted cluster..... 28

LIST OF FIGURES – CONTINUED

Figure Page

3.12 Representative HPLC Chromatrograms used to quantify GTPase activity..... 29

3.13 Plot of integrated intensities of the GDP peak versus time from HPLC chromatograms for $HydF^{EG}$..... 29

3.14 Plot of integrated intensities of the GDP peak versus time from HPLC chromatograms for $HydF^{\Delta EG}$ stripped of Fe..... 30

3.15 Plot of integrated intensities of the GDP peak versus time from HPLC chromatograms for $HydF^{\Delta EG}$ reconstituted..... 31

3.16 Plot of integrated intensities of the GDP peak versus time from HPLC chromatograms for $HydF^{\Delta EG}$ (1μM) in the presence of $HydA^{\Delta EFG}$ (10 μM)..... 32

3.17 Plot of integrated intensities of the GDP peak versus time from HPLC chromatograms for $HydF^{\Delta EG}$ (1 μM) in the presence of $HydG^{EF}$ (10 μM)..... 33

3.18 Plot of integrated intensities of GDP peak versus time from HPLC chromatograms for Hyd F^{EG} (1μM) in the presence of $HydE^{FG}$ (10 μM)..... 34

3.19 Plot of integrated intensities of the GDP peak versus time from HPLC chromatograms for $HydF(S26A)^{\Delta EG}$ (4 μM)..... 36

3.20 Plot of integrated intensities of the GDP peak versus time from HPLC chromatograms for $HydF(S26A)^{EG}$ (4 μM)..... 36

3.21 Normalized chromatogram of $HydF(S26A)^{EG}$ compared to $HydF(S26A)^{\Delta EG}$..... 37

LIST OF FIGURES – CONTINUED

Figure Page

3.22 Plot of integrated intensities of the GDP peak versus time from HPLC chromatograms for HydF(C353S)$^{\Delta EG}$ (70 μM)..... 38

4.1 GTP binding by HypB from *M. jannaschii* showing Mg^{2+} and GTP coordination..... 42

4.2 GTP binding by MnmE from *E. coli*, showing Mg^{2+} and GDP-AlF_4^- coordination..... 42

LIST OF SCHEMES

Scheme Page

1.1 Reaction Steps of Biotin Snythase..... 9

ABSTRACT

The [FeFe]-hydrogenase contains an unusual active-site cluster, the H-cluster, composed of a [4Fe-4S] cluster bridged to a 2Fe subunit coordinated by CO, CN^-, and a nonprotein bridging dithiolate. Three accessory proteins, HydE, HydF, and HydG are required for maturation of the H-cluster. It has been proposed that the GTP-hydrolyzing protein HydF acts as a scaffold for assembly of the [2Fe] subcluster, which is then transferred to hydrogenase to produce the active enzyme[McGlynn, S.M.; Shepard, E.M.; Winslow, M.A.; Naumov, A.V.; Duschene, K.S.; Posewitz, M.C.; Broderick, W.E.; Broderick, J.B.; Peters, J.W. *FEBS Lett.* **2008,** *582,* 2183.]. The precise roles of HydE, HydF, and HydG in this process, however, remain unclear. The overall goal of this work is to study the role of HydF in hydrogenase maturation. *In vivo* studies have identified specific amino acid residues of HydF necessary for production of active hydrogenase [King, P.W.; Posewitz, M.C.; Ghirardi, M.L.; Seibert, M. *J Bacteriol.* **2006,** *188,* 2163.]. The objectives of this study were to: 1) investigate the involvement of each of these amino acid residues on the GTP hydrolyzing ability of HydF 2) examine the effects of structural and accessory hydrogenase proteins on rate of GTP hydrolysis 3) examine the importance of [Fe-S] cluster in HydF GTPase activity. GTPase assays were analyzed by high performance liquid chromatography (HPLC). The results indicate mutations to conserved glycine residues in the GTP binding loop, and a potential iron ligand for the [Fe-S] cluster are deleterious to GTPase activity. Another mutation in the GTP binding loop involved in Mg^{2+} coordination appears to have little effect on the rate of GTP hydrolysis. The two accessory proteins HydE and HydG increased GTPase activity, while the hydrogenase structural protein (HydA) appears to have little effect, supporting the suggestion that HydF acts as a scaffold. The presence or absence of an iron-sulfur cluster does not significantly affect GTPase activity. Together, these results suggest GTP hydrolysis does not play a role in transfer of activating elements to hydrogenase, but does play a role in hydrogenase maturation.

INTRODUCTION

The global hydrogen cycle is dependent on microorganisms for the reduction of protons and oxidation of molecular hydrogen (1). Hydrogenases have evolved to efficiently catalyze the reversible oxidation of hydrogen, and such facile reactions have implications for the use of hydrogen as a fuel source (2). Three phylogenetically unrelated metalloenzymes, the [NiFe]-, [FeFe]-, and [Fe]-hydrogenases, are involved in the hydrogen cycle (3). Two of these, the [NiFe]- and the [FeFe]-hydrogenases, specifically catalyze the reversible oxidation of hydrogen, although typically the [NiFe]-hydrogenase oxidizes hydrogen while the [FeFe]-hydrogenases are H_2-forming (3). The [Fe]-hydrogenase, in contrast, catalyzes the dehydrogenation of methylenetetrahydro-methanopterin.

The [NiFe]- and [FeFe]-hydrogenases, whose names reflect the active site metal content, require several accessory proteins to assemble their complicated active sites and metal clusters. As described in the following section, biological [Fe-S] clusters may be assembled by general purpose cellular machinery, but the active site of both the [Fe-Fe]- and [Ni-Fe]-hydrogenases include potentially toxic CO and CN^- ligands that are not abundant *in vivo*, and so several specialized proteins are required for synthesis and delivery of these ligands (4). The [NiFe] enzyme requires seven accessory proteins, while the [FeFe] enzyme requires three; named HydE, HydF, and HydG (5). The aim of this work is to elucidate the specific roles of the [FeFe]-hydrogenase accessory proteins

HydE, HydF, and HydG in producing the mature, catalytically active structural enzyme, HydA.

Iron Sulfur Clusters

Iron-sulfur clusters are known to be pervasive in living organisms, and understanding their structures, functions, and assembly continues to be an active area of research (6). Iron-sulfur clusters are able to self-assemble in apo-proteins under reducing conditions when S^{2-} and Fe^{2+}/Fe^{3+} are supplied, however, *in vivo* multiple proteins are required to properly form the desired [Fe-S] clusters (7). Organism requirements vary, but typically a Nif (nitrogen fixation), Isc (iron sulfur cluster), or Suf (sulfur utilization factor) system is utilized for [Fe-S] cluster formation (8). These systems use cysteine desulfurases to provide sulfide, and require a scaffold protein for cluster construction (8).

In principle and occasionally in practice, a [2Fe-2S] cluster acts as the fundamental [Fe-S] cluster from which more complicated clusters may be constructed (6). For example, the [4Fe-4S] cubane structure can be obtained upon reductive coupling of two [2Fe-2S] clusters (6). Iron-sulfur clusters are considered to be ancient structures in the history of life, and the first living organisms may have based their iron-sulfur cluster structure on minerals that incorporate the two elements (9). The prevalence of [Fe-S] clusters across phylogeny indicate their ancient origins, and use of [Fe-S] clusters in catalysis has been postulated to start abiotically on iron-sulfur containing minerals, such as mackinawite, which resembles the hydrogenase active site structure (10). This

longstanding presence of [Fe-S] clusters in biology may have resulted in a variety of catalytic and functional capabilities, as described below.

Iron-sulfur clusters commonly participate in electron transfer, and this was their first known function (6). Additional roles show [Fe-S] clusters are not limited to electron transfer, and are involved in such functions as dimer formation (11) and protein stabilization (12). Additionally, clusters can coordinate and activate substrates for catalysis; examples include the radical SAM enzymes (13) which bind *S*-adenosyl methionine to a unique iron site prior to its reductive cleavage, and nitrogenase and hydrogenase, which bind and activate N_2 and H_2, respectively, at complex metal centers (11, 4). Iron-sulfur clusters are also involved in regulatory activities, with changes in cluster composition or oxidation state as a signal for regulating gene expression (14). Clusters participate in protein structure stabilization (12), and may be involved in iron storage (8).

[NiFe]-Hydrogenase

Although the [NiFe]- and [FeFe]-hydrogenases have separate evolutionary lineages, their shared hydrogen oxidation/reduction ability and active site structural likenesses suggest that similarities may exist in the synthesis of their respective active sites. The nickel and iron of the [NiFe]-hydrogenase are coordinated by four cysteines, including one bridging cysteine, as determined by cyrstallographic characterization (15). The nonprotein bridging ligand composition is uncertain (16); sulfide (17), and peroxo (18) ligands have been proposed; this is modeled as an oxygen (19) in Figure 1.1. The

nickel-iron center, two CN^-, and one CO ligand of the active site of *Desulfovibrio gigas* can be seen in Figure 1.1.

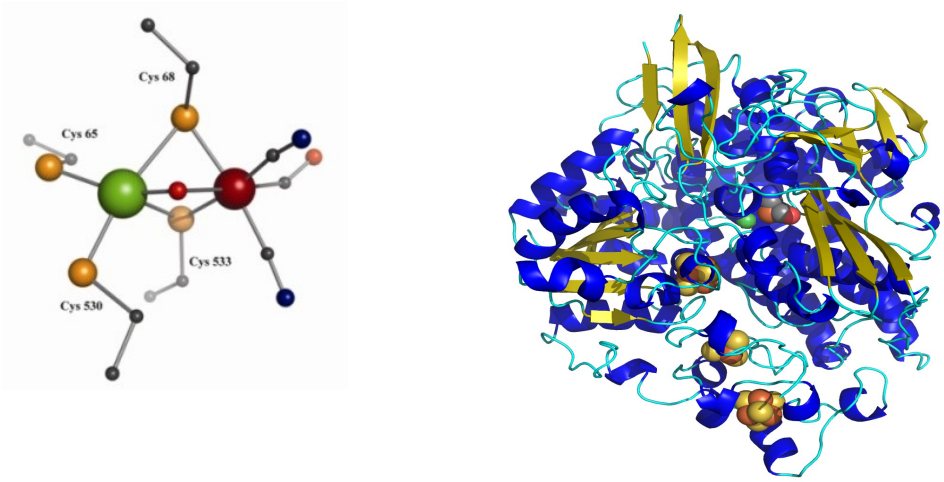

Figure 1.1 Active site and overall structure of the [NiFe]-hydrogenase from *D. gigas* (15). Green corresponds to nickel, rust to iron, yellow to sulfur, black to carbon, blue to nitrogen, red to oxygen, image from (20), PDB ID: 2FRV.

Extensive study of the [NiFe]-hydrogenase implicates a host of accessory proteins necessary for active site assembly, and several more responsible for the construction of iron-sulfur clusters found in the body of the protein (4). Housekeeping Isc proteins are involved in the assembly of [4Fe-4S] clusters, and an ABC transporter responsible for Ni transport and siderophores responsible for Fe transport are involved in the delivery of metal to the apo-protein (4). HypE and HypF catalyze CN^- synthesis from carbamoyl phosphate (21). HypC and HypD appear to be involved in Fe insertion and the binding of the CN^- ligand, however, the mechanistic details of this process are not entirely clear (22). HypB and HypA both have Ni binding ability and could be involved in Ni insertion (4). In addition to all these chaperones, several [NiFe]-hydrogenases require a proteolytic enzyme to remove a portion of the C-terminus before the holoprotein is complete (4).

[FeFe]-Hydrogenase

The [FeFe]-hydrogenase enzymes (HydA) from *Clostridium pasteurianum* (CpI) (23) and from *Desulfovibrio desulfuricans* (DdH) (24) have been structurally characterized at 1.39 Å and 1.6 Å resolution, respectively , seen in Figure 1.2. The mushroom shaped enzyme from CpI has four [Fe-S] clusters in addition to the active site. The clusters of the protein are within 8 to 11 Å of each other, reasonable distances for electron transfer. The truncated DdH enzyme also has FeS clusters located in a manner suggestive of electron transport. The CpI C-terminus is similar to the DdH small subunit, as both wrap around a cleft near the active site (25).

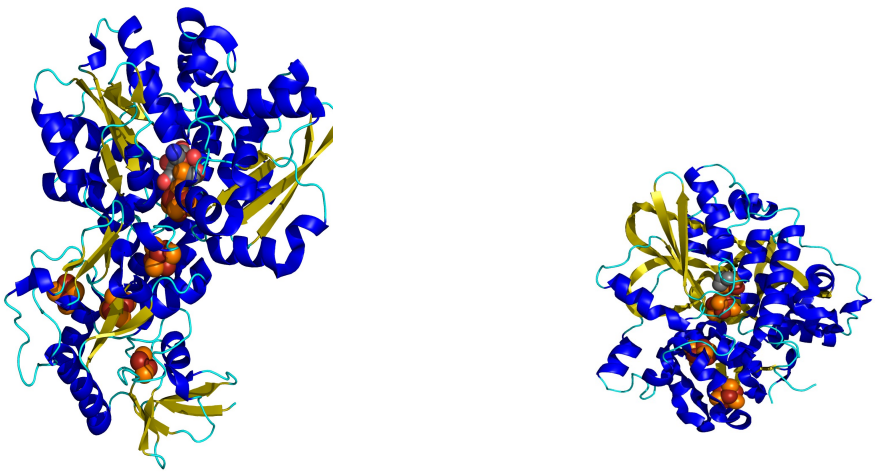

Figure 1.2 Crystal structures of CpI, (PDB ID 3C8Y, 1.39 Å (23)) and DdH (PDB ID 1HFE)(1.6 Å) demonstrating location of [Fe-S] clusters including the active site (24). The [Fe-S] clusters are shown in rust and yellow.

The [FeFe]-hydrogenase active site, called the H-cluster, involves a cubane [4Fe-4S] cluster connected to a 2Fe subcluster through a bridging cysteine. The 2Fe subcluster is additionally ligated by 5 CO/CN^- molecules, a water molecule, and a nonprotein dithiolate ligand bridging the two Fe centers. Figure 1.3 shows the hydrogenase active site H-cluster. The precise identity of the dithiolate ligand is not yet defined; although initially modeled as a propane dithiolate, further investigation suggested a dithiomethylamine with a nitrogen as the bridgehead atom to act as a base for heterolytic cleavage (26). More recent computational studies have indicated a dithiomethylether model fits crystallographic data best as compared to several other ligands, including propane dithiolate and dithiomethylamine (23). The origin of this nonprotein ligand, as well as the derivation of CO and CN^- ligands are unknown, making it more difficult to determine possible pathways for assembly. For the [NiFe]-hydrogenase, the synthesis of CN^- is proposed to result from the interactions of two Hyp proteins (21), but no such analogous proteins have been found in organisms which express [FeFe]-hydrogenase.

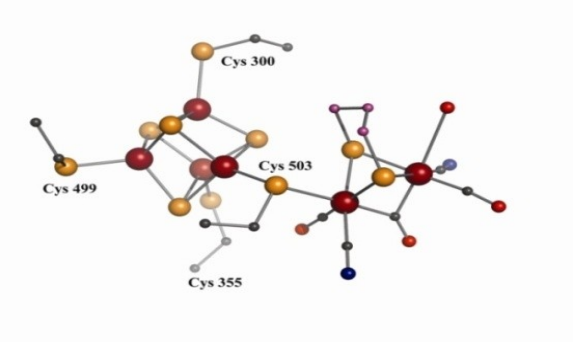

Figure 1.3 Active site of the *C. pasteurianum* [FeFe] Hydrogenase, from (20).

Using a model such as $Fe_2(S_2C_3H_6)(CO)_4(PMe_3)_2$ to represent the [2Fe-2S] cluster of the hydrogenase active site, Zhou and coworkers examined the mechanism of hydrogen reduction by density functional theory (27). Based on previous evidence that a CO ligand bridges the two iron atoms, a theory was proposed whereby the CO moves to the distal Fe when a μ-hydride is acquired. Comparison of oxidized and CO inhibited forms of *C. pasteurianum* point toward the distal Fe being involved in hydrogen reduction (28). The hydride would then abstract a hydrogen atom attached to one of the bridging sulfur atoms, and the weakly bound hydrogens would coordinate to just one of the Fe atoms present. The addition of an electron, perhaps from the [4Fe-4S] cluster to the proximal iron would further weaken the η^2H_2 – Fe bond, strengthening the H-H bond. A few assumptions are made with these calculations, such as the identity of the dithiolate ligand, and the unusual dual-coordinated H_2. However, such $\eta^{2-}H_2$ chemistry is precedented, most notably in the [NiFe]-hydrogenase (27).

Proteins essential for hydrogenase maturation were first identified in 2004 when random mutations in *Chlamydomonas reinhardtii* were screened for hydrogen production (5). A mutation in *hydEF* pinpointed the gene product as essential to hydrogen production, and homologues for HydE, HydF, and a neighboring HydG were found in most sequenced [FeFe]-hydrogenases (5). Sequence analysis indicated the HydE and HydG proteins belong to the Radical SAM superfamily, and the HydF had a domain predicted to have GTPase activity. When HydE, HydF, and HydG are present, active HydA can be heterologously expressed (29). Hydrogen evolving assays indicated no activity with HydA grown in the absence of HydE, HydF, and HydG, but HydA could be

activated after interacting with three coexpressed accessory proteins; HydE, HydF, and HydG (30). Such a small number of helper proteins is impressive considering the complicated assembly of the [NiFe] center, which requires seven distinct proteins (31). All three accessory proteins appear to have [Fe-S] clusters, but the precise role of each protein has not been determined (5). McGlynn *et al.* demonstrated HydF coexpressed with HydE and HydG ($HydF^{EG}$) is capable of activating $HydA^{\Delta EFG}$ (HydA grown in the absence of HydE, HydF, and HydG) (30). $HydA^{\Delta EFG}$ cannot be activated by $HydF^{\Delta EG}$ (HydF grown in the absence of HydE and HydG), indicating HydF obtains some activating element through interacting with HydE and HydG, and then transfers this to $HydA^{\Delta EFG}$. Recent work has indicated HydA expressed in the absence of accessory proteins contains the [4Fe-4S] cluster but lacks the 2Fe subcluster of the active site (32).

Hydrogenase Accessory Proteins

Radical SAM Enzymes HydE and HydG

Sequence analysis has revealed the HydE and HydG proteins are radical *S*-adenosyl methionine (SAM) enzymes, each containing the conserved CX_3CX_2C motif found in this family of proteins (5). Within the superfamily, this motif binds a redox active site-differentiated [4Fe-4S] cluster that coordinates SAM at the unique iron (13) . Reductive cleavage of SAM results in a 5'-deoxyadenosyl radical and methionine (33). The radical then abstracts a hydrogen atom from the substrate, creating a new radical that can be involved in several different types of chemistry. Radical SAM enzymes catalyze a variety of reactions, including the formation of glycyl radicals, isomerization reactions,

and sulfur insertions (8). The initial discovery of the radical SAM superfamily identified over 500 members (13), and even though several similarities are found within radical SAM enzymes, the chemistry varies considerably between subfamilies.

Biotin synthase is an example of a radical SAM enzyme that shares sequence and structural similarity with HydE (34). Biotin synthase (BioB) catalyzes a sulfur insertion into dethiobiotin to form biotin (Scheme 1.1). Spectroscopic characterization of biotin synthase indicates one [4Fe-4S] cluster and one [2Fe-2S] cluster are bound by the protein (35). The sulfur source for the enzyme has not been decisively determined, and has been speculated to be the [2Fe-2S] cluster (35), explaining low turnover rates observed *in vitro* by requiring cluster reassembly after each reaction. Scheme 1.1 shows the biotin synthase reaction scheme. Considering the similarities between HydE and BioB, we hypothesize that HydE may catalyze sulfur insertion reactions required for the synthesis of the bridging dithiolate ligand of the H-cluster.

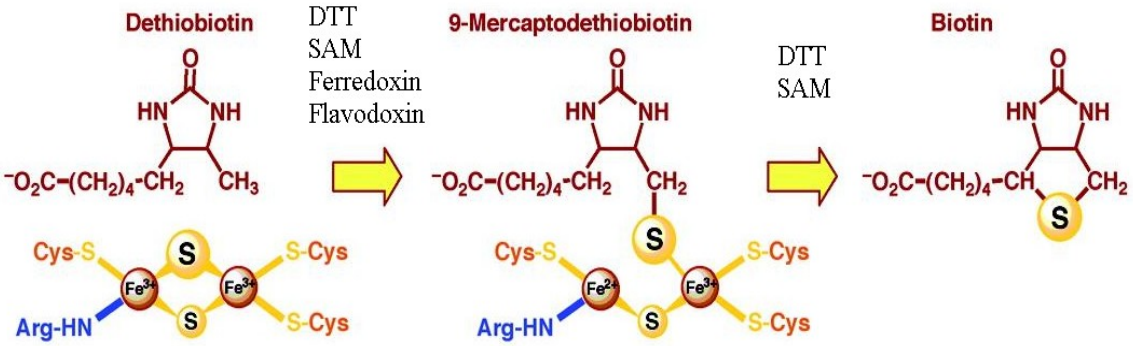

Scheme 1.1 Reaction Steps of Biotin Synthase, modified from (36)

The crystal structure of HydE from *Thermotoga maritima* has been solved (34), confirming a triose-phosphate isomerase (TIM) type $(\alpha/\beta)_8$ barrel structure common to radical SAM enzymes, as well as a bound [4Fe-4S] cluster. In the work by King *et al.* identifying the accessory proteins necessary to assemble an active [FeFe]-hydrogenase, mutations of the conserved radical SAM cluster-binding motif in HydE resulted in a loss of H_2 production in whole cell extracts, signaling an important role for radical SAM chemistry in the maturation of HydA (37).

Less still is known about HydG, for which no crystal structure has been determined. Mutations to the radical SAM binding motif and another [Fe-S] binding motif in HydG also resulted in significant loss of hydrogen production in whole cell extracts (37). HydG shares sequence similarity with another radical SAM enzyme, ThiH, a tyrosine lyase (38). The breakdown of tyrosine by ThiH results in p-cresol and dehydroglycine, and recently Pilet and coworkers showed increased production of p-cresol with HydG when tyrosine was present (38). A pathway for the products have not yet been determined, but the results suggest tyrosine may be the source of precursor molecules necessary for the non-protein ligands in the hydrogenase active site. In a hypothesis published in 2006, Peters *et al.* anticipated a small molecule precursor forming the dithiolate linkage of the H-cluster from interactions with HydE or HydG (39) that could reasonably come from a tyrosine breakdown product like dehydroglycine. The theory also suggested the cubane [Fe-S] cluster of the active site is already present in the immature HydA, and that HydF may act as a scaffold. Since then, both of these predictions have been experimentally verified (32, 30).

HydF

The third accessory protein, HydF, has been identified as a GTPase based on the presence of several conserved domains common to GTP binding proteins and later through detection of GTP hydrolysis (40). The conserved domains include a Walker A P loop responsible for binding the phosphate groups of GTP in the N-terminus, a Walker B Mg^{2+} binding loop in the C-terminus, and a conserved [Fe-S] cluster binding motif, $CxHx_{46-53}CxxC$ (37). Three conserved cysteines could play a role in [Fe-S] cluster coordination, and there is some evidence that the fourth Fe in *Thermotoga maratima* is coordinated by a histidine ligand (40).

NTPase-catalyzed hydrolysis can couple with an event like a metal transfer, seen with Ni insertion in HypB with the [NiFe]-hydrogenase and UreG in urease (41), as well as with the iron protein NifH inserting the FeMo-cofactor into nitrogenase (42). With similar ligands such as CO and CN^- found in both the [NiFe]- and [FeFe]- hydrogenases (4), it is interesting to consider whether the [NiFe] hydrogenase GTP protein, HypB, may have similarities to HydF. HypB has been implicated in Ni coordination and transport (43), and this protein has been crystallized and appears to dimerize upon the addition of GTP (44). It is tempting to speculate on the similarities of HypB and HydF, however it is important to remember they come from phylogenetically distinct lines and appear to have different mechanisms for nonprotein ligand insertion.

It was recently demonstrated that HydF expressed in the background of HydE and HydG ($HydF^{EG}$) was competent to activate $HydA^{\Delta EFG}$ (30). Furthermore, the activity of $HydA^{\Delta EFG}$ in the presence of $HydF^{EG}$ was not enhanced by GTP (30). These findings indicate that HydF, after interacting with HydE and HydG, is responsible for transferring

an activating component to HydA. Since the presence of GTP does not improve the activity for HydA, it seems HydF hydrolysis of GTP is not coupled to a transfer of ligands or metal into HydA, and thus may be utilized elsewhere in the cluster maturation process. *Clostridium acetobutylicum* HydF GTPase activity appears to be dependent on monovalent cation size, showing greatest activity in the presence of potassium (Shepard et al., in preparation). Salt dependent activity has been observed previously with another GTPase from *E. coli*, MnmE, and may be attributed to the stabilization of a β-phosphate of GTP by the cation in addition to Mg^{2+} bound by the Walker B loop and a positively charged lysine residue in the Walker A P loop (45). Changing conserved residues in the Walker A P loop (G19A, G24A, and S26A) resulted in the loss of hydrogenase activity in whole cell extracts (37). Changing the C353 and C356 to serine also resulted in a loss of hydrogen production in whole cell extracts.

GTPase activity of HydF was first reported in *T. maritima* with a k_{cat} of 0.03 min^{-1} (40). More recent work in our lab has indicated that *C. acetobutylicum* HydF has higher turnover rates, around 2.0 min^{-1} (manuscript in preparation). Using HydF as a reporter, it is possible to probe the interactions of this potential scaffold with the hydrogenase protein as well as the other two accessory proteins, HydE and HydG. GTPase activity can also be examined with respect to the presence or absence of [Fe-S] cluster content in the protein as well as the role of individual amino acids in GTP hydrolysis. Each interaction offers a wealth of insight into the mechanism of hydrogenase maturation.

MATERIALS AND METHODS

Cell Growth

Culturing of cells was carried out at 37°C using autoclaved media and appropriate antibiotics (50 μg/mL ampicillin for HydE, 30 μg/mL kanamycin for HydF, and 50 μg/mL streptomycin for HydG). Cells containing HydE required ampicillin, HydF required kanamycin, and HydG required streptomycin. Additional proteins expressed with the enzyme of interest is noted by their presence in the superscript of the protein name, for example $HydF^{EG}$ indicates HydF coexpressed with HydE and HydG, and then purified. The Δ symbol in the superscript indicates the absence of additionally expressed proteins. Cells were plated from glycerol stocks onto Luria Broth (LB) plates and grown overnight. An overnight culture was prepared by inoculation of 50 mL of 50mM phosphate buffered LB (pH 7.5, with appropriate antibiotics) was grown overnight with shaking at 240 rpm. The overnight growth (six 7.5 mL aliquots) was then transferred to six 1.5 L flasks of phosphate buffered LB pH 7.5 (including appropriate antibiotics), supplemented with 5g/L glucose and grown with shaking at 240 rpm to an optical density of 0.5-0.6 at 600 nm. Once the desired OD was reached the cells were induced with IPTG (1mM final concentration) and supplemented with 0.06 g/L ferrous ammonium sulfate. Cells were allowed to grow with shaking for an additional 2 hours, then were allowed to cool on the benchtop for 60 minutes before being sparged with nitrogen at 4ºC overnight. The cells were then centrifuged at 8,000 rpm for 10 minutes at 4ºC. The supernatant was decanted and the cell pellets were frozen in liquid N_2 and stored at -80ºC.

Protein Purification

All purification procedures were carried out under strictly anaerobic conditions unless otherwise noted. Cells were mixed with two volumes (e.g. 20 mL per 10g cells) of lysis buffer, composed of Buffer A (50mM HEPES, 0.5M KCl, 5% glycerol, 10 mM imidazole, pH 7.4), 1% Triton X-100, 5 μM PMSF, 9 mg/50mL lysozyme, 100 mg/50mL $MgCl_2$ and trace amounts of RNAse A and DNAse I. The lysis was carried out over the course of an hour, with repetitive syringing of the suspension, then put in centrifuge tubes. The centrifuge tubes with screw caps and O-rings were removed from the anaerobic chamber and centrifuged at 4°C at 18,000 rpm for 30 minutes. The tubes were returned to the Coy chamber and the supernatant was loaded onto a Ni^{2+}/His immobilized metal affinity chromatography (IMAC) column (Pharmacia) previously equilibrated with 10 column volumes Buffer A. An FPLC was used for column loading, washing, and elution. After loading supernatant onto the column using a superloop, the column was washed with 10 column volumes Buffer A (50mM HEPES, 0.5M KCl, 5% glycerol, 10 mM imidazole, pH 7.4) at 4 mL/min before eluting protein. Absorbance at 280 nm (to observe protein) and 426 nm (to observe Fe) was monitored during elution. A step gradient was used to elute protein by increasing imidazole concentration from 10 mM imidazole for a wash to 50 mM imidazole for 5 column volumes, to 100 mM imidazole for 5 column volumes, to 250 mM imidazole for 5 column volumes, to 500 mM imidazole for 10 column volumes, all at 2 mL/min. Fractions (1.8 mL) were collected at 100 mM, 250 mM, and 500 mM imidazole elution concentrations. Samples

of each fraction were run on SDS-PAGE to determine the purity level of the desired protein, and then were pooled and dialyzed vs a 1000-fold excess buffer (50mM HEPES, 0.5 M KCl, 5% glycerol, pH 7.4) for 5 hours under anaerobic conditions. Protein concentration was carried out by ultrafiltration with a YM-10 membrane. Protein was then stored at -80°C in screwcap vials.

Iron-Depleted and Reconstituted HydF

Metal depletion and reconstitution were performed in a Coy anaerobic chamber. $HydF^{\Delta EG}$ (160 μM) was stripped of metal content by incubation overnight with 25 mM EDTA in 50 mM HEPES, 0.5 M KCl, 5% glycerol, pH 7.4 buffer. After overnight incubation, the sample was extensively dialyzed (in the same buffer lacking EDTA) for removal of the chelating agent.

Reconstitution of $HydF^{\Delta EG}$ was achieved by incubating the enzyme with 5mM DTT in 50 mM HEPES, 0.5 M KCl, 5% glycerol, then the addition of 6-fold excess of $FeCl_3$ with gentle stirring. After 20 minutes, 6-fold excess of Na_2S was added to the reconstitution mixture, and the solution was allowed to stir for another 2.5 hours. After the reconstitution period, EDTA was added to a final concentration of 2 mM for 30 minutes. The mixture was then centrifuged, and the supernatant was run over a Sephadex G-25 column for removal of excess ions, and the protein was then concentrated using an Amicon YM-10 spin concentrator. UV-Vis was used to determine [Fe-S] presence or absence using a Cary 6000i UV/Vis spectrophotometer (Varian).

Quantifying Protein and Iron Content

Protein concentration was determined by Bradford assay with bovine serum albumin (BSA) as a standard. Seven standards were prepared, ranging in concentration from 0 to 6 μg/mL BSA. A 1:100 dilution of the unknown protein sample was made, then 3 to 6 samples were prepared with further dilution of the protein sample, typically ranging from 10 to 60 μL sample into 0.8 mL final volume prior to the addition of dye. Bradford Dye (200 μL) was then added to the standards and samples, bringing the total volume of each sample to 1 mL. The samples were then incubated at room temperature for 60 minutes, and the absorbance was measured at 595 nm. Iron content was determined by an iron assay (46). Six 1 mL dilutions of an Fe standard ranging from 0 to 2 μg/mL were prepared. Protein samples (200 μL) were diluted to 1 mL with water, then 2 3-fold and 2 6-fold dilutions were made with a final sample volume of 1 mL for each dilution. Once dilutions were prepared, 500 μL Reagent A (1:1 1.2M HCl, 4.5% $KMnO_4$) was added to each sample, and all samples were gently vortexed and incubated in a $60^{O}C$ water bath for 2 hours. After 2 hours, 100 μL Reagent B (5M ammonium acetate, 2 M ascorbic acid, 15 mM neocuprine, 6 mM ferrozine) was added, and samples and standards were incubated at room temperature for 30 minutes. The absorbance was then read at 562 nm (with reference wavelength at 900 nm).

GTPase Assays and HPLC Analysis

All GTPase assays were performed at 30ºC. Buffer (50 mM HEPES, 0.5 M KCl, 5% glycerol pH 7.4), $MgCl_2$, DTT, and GTP were sequentially added to a 1.5 mL Eppendorf tube. The tube was then incubated in a warming plate at 30ºC for 5 minutes. Then the GTPase protein (HydF) and any secondary protein was added and the timer was started. The final concentrations of $MgCl_2$, DTT, and GTP in the assay were 2mM. HydF protein concentration ranged from 1 to 70 μM. At the desired timepoint, two 50 μL aliquots were removed from the reaction mixture and 3 μL 1M HCl was added and then put in liquid nitrogen to quench the reaction.

Samples were prepared for HPLC by submersion into boiling water for 45 seconds. They were then centrifuged at 13,000 rpm for 10 minutes at 4ºC. The supernatant was removed and put over an Amicon spin filter membrane (MWCO 3,000 Da) and centrifuged at 4ºC for 60 minutes. Samples were then stored at -80ºC.

All samples were run on HPLC using HPLC grade solvents, with the column maintained at 34ºC and eluent monitored at 254nm. The Waters Spherisorb 5 μM C18 4.6 x 150 mm ODS2 reverse phase column was equilibrated with 10 column volumes Buffer B (50 mM sodium phosphate buffer, 10 mM tetrabutyl ammonium bromide, pH 6.5). Samples were eluted with a program running 4% acetonitrile, 96% Buffer B, at 0.75 mL/ min for 10 minutes, before going to 100% Buffer B at 1 mL/min. The GDP peak elutes first at approximately 5.5 minutes, followed by the GTP peak at approximately 8 minutes. Sample injection volumes of 10 μL were used.

Peak integration was performed using Origin 8.0 (OriginLab, Northampton, MA). For controls, both the GTP and GDP peak were integrated separately, and an average GDP and GDP + GTP peak area were determined. For a sample, the average control GDP peak area was subtracted from the sample GDP peak area. The resulting area was divided by the control GDP + GTP peak area to determine the percent difference between the control and the sample. To determine the concentration of GDP, the percent difference was multiplied by 2000 μM (the initial concentration of GTP). Once concentration of GDP for each time point was calculated, a graph of [GDP] vs. time was plotted, and a linear regression was calculated. The slope of the line then corresponded to μmol $min^{-1}L^{-1}$ GDP. From this number k_{cat} was determined.

DATA AND RESULTS

Protein Purification and Characterization

After protein purification, samples of each fraction collected were run by SDS-PAGE to confirm protein molecular weight and assess purity. The following figures show representative chromatograms from purifications and SDS-PAGE gels for each protein purified. Selected fractions were dialyzed, concentrated and characterized for concentration and Fe content before being used in assays.

HydF

Nine liter cultures of HydF$^{\Delta EG}$-expressing *E. coli* typically resulted in 30 to 35 grams of cells. A 15 g purification would result in approximately 100 mg of purified protein, with iron numbers ranging from 0.4 to 1.2 Fe/protein. The protein eluted from the column at 100 to 500 mM imidazole, with purity estimated at ~90% (Figure 3.1).

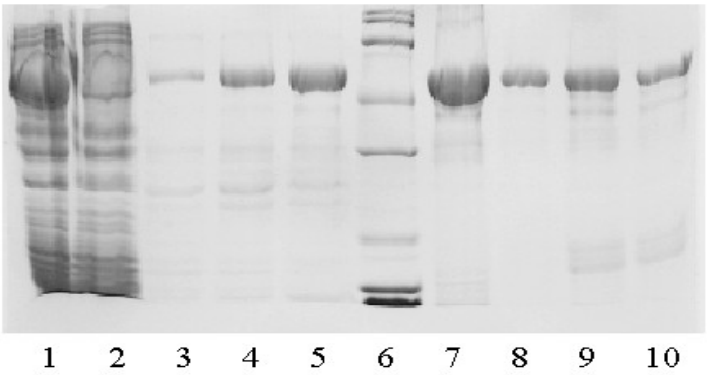

Figure 3.1 SDS-PAGE analysis of fractions from a HydF$^{\Delta EG}$ purification. Aliquots of fractions (10μL each) of a sample were loaded in each lane. Lane 1, cell extract; Lane 2, flow through; Lanes 3, 4, and 5, 100 mM imidazole elution; Lane 6, molecular weight marker; Lanes 7 and 8, 250 mM imidazole elution; Lanes 9 and 10, 500 mM imidazole elution. The molecular weight marker shows bands (from top to bottom) with molecular weights of 200,000 Da; 116,250 Da; 97,400 Da; 66,200 Da; 45,000 Da; 31,000 Da; 21,500 Da; 14,400 Da; and 6,500 Da respectively. HydF is slightly above 45,000 Da (HydF MW= 47,268 Da) in lanes 3-5 and 7-10.

Nine liter cultures of HydF^{EG}-expressing *E. coli* typically resulted in 30 to 35 grams of cells with approximately 30 g used for a purification. A 30 g purification would result in approximately 20 mg of purified protein, with iron numbers ranging from 0.5 to 1.4 Fe/protein. HydF^{EG} elutes at 100 to 250 mM imidazole and is estimated to be greater than 95% pure (Figure 3.2).

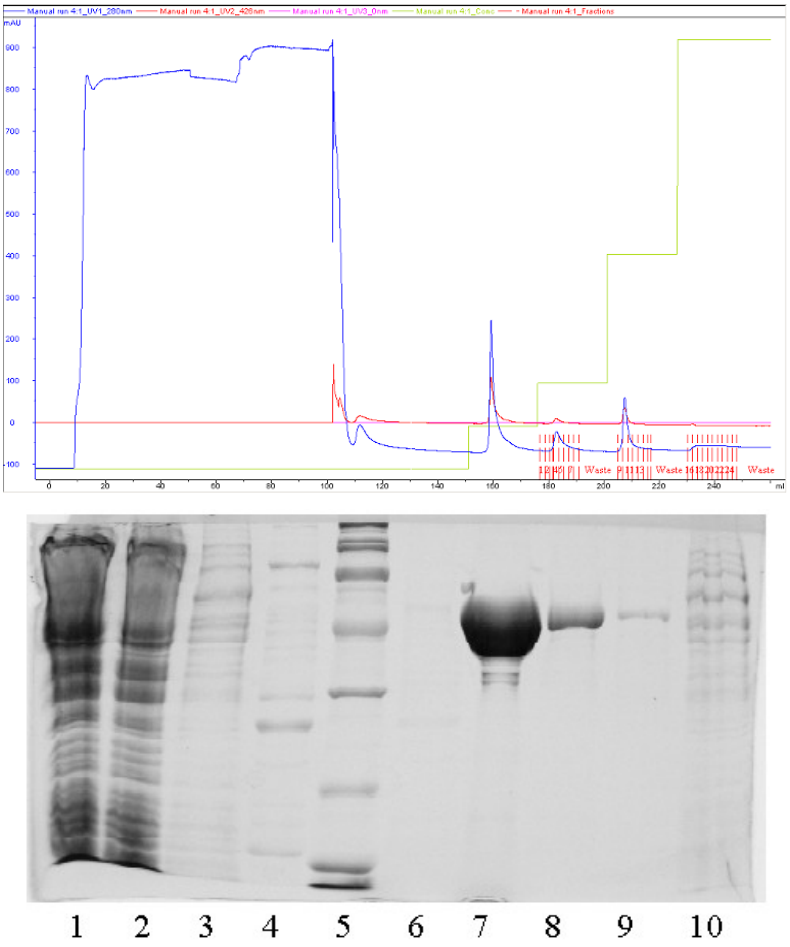

Figure 3.2 Purification of HydF^{EG}. Chromatogram (top) of HydF^{EG} purification, showing A_{280} in blue for monitoring protein, and A_{426} in red for monitoring [Fe-S] cluster. SDS-PAGE analysis of fractions (bottom) from a HydF^{EG} purification. Aliquots of fractions (15µL each) were loaded in each lane . Lane 1, cell extract; Lane 2, flow through; Lanes 3 and 4, 100 mM imidazole elution; Lane 5 MW Marker; Lanes 6, 7, and 8, 250 mM imidazole elution; Lane 9, 500 mM imidazole elution; Lane 10, 10 mM imidazole wash.

HydG

Nine liter cultures of HydG$^{\Delta EF}$-expressing *E. coli* typically resulted in 30 to 35 grams of cells, with approximately 15 g used for a purification. A 15 g purification would result in approximately 50 mg of purified protein, with iron numbers ranging from 1.3 to 2.8 Fe/protein. The protein eluted from the IMAC column at 100 to 500 mM imidazole, with an estimated purity of greater than 90% (Figure 3.3).

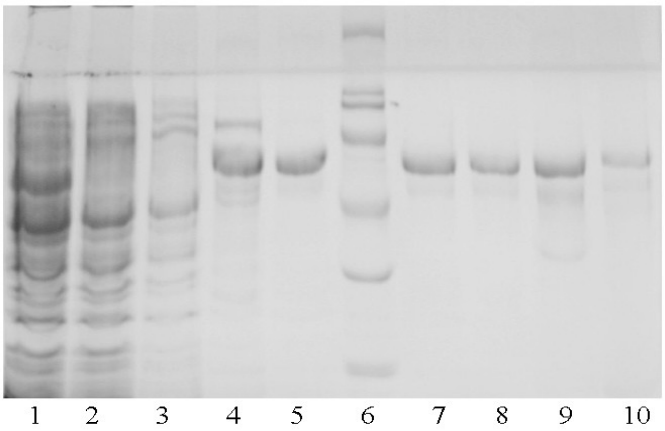

Figure 3.3 SDS-PAGE analysis of fractions from a HydG$^{\Delta EF}$ purification. Aliquots of fractions (10 µL each) were loaded in each lane. Lane 1, cell extract; Lane 2 flow through; Lane 3, 10 mM imidazole wash; Lanes 4, 5, 7, and 8 are from fractions collected at 100 mM imidazole elution; Lane 6, molecular weight marker; Lane 9, 250 mM imidazole elution; Lane 10, 500 mM imidazole elution. HydG appears at approximately 55,200 Da.

A nine liter culture of HydG^{EF}-expressing *E. coli* resulted in 30 grams of cells, all of which were utilized in one purification. The 30 g purification resulted in approximately 70 mg of purified protein, with an iron numbers of 1.38 ± 0.03 Fe/protein. The protein eluted from the IMAC column at 100 to 500 mM imidazole with purity estimated at ~90% (Figure 3.4).

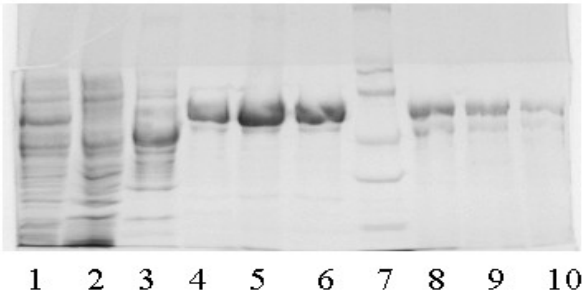

Figure 3.4 SDS-PAGE analysis of fractions from a $HydG^{EF}$ purification. Aliquots of fractions (10 μL each) were loaded in each lane. Lane 1, cell extract; Lane 2, flow through; Lane 3, fraction from 50 mM imidazole elution; Lanes 4, 5 and 6, fractions from 100 mM imidazole elution; Lane 7, molecular weight marker; Lanes 8, 9, and 10, fractions from 500 mM imidazole elution.

HydE

Nine liter cultures of $HydE^{FG}$-expressing *E. coli* typically resulted in 30 to 35 grams of cells, with approximately 30 g used for a purification. A 30 g cell pellet for purification would result in approximately 15 mg of purified protein. No iron content was determined for $HydE^{FG}$ as such small amounts of protein were obtained that it was only used for assays. $HydE^{FG}$ also precipitated easily and was difficult to concentrate. At ~50 μM, $HydE^{FG}$ did appear to have a faint brown color, characteristic of an [Fe-S] cluster. $HydE^{FG}$ eluted from the IMAC column at 100 to 250 mM imidazole with purity estimated at ~80% (Figure 3.5).

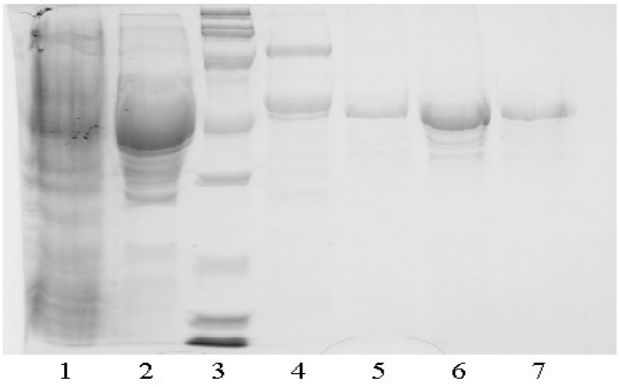

Figure 3.5 SDS-PAGE analysis of fractions from a $HydE^{FG}$ purification. Aliquots of fractions (15 μL each) were loaded in each lane. Lane 1, cell extract; Lane 2, fraction from 50 mM imidazole elution; Lane 3, molecular weight marker; Lane 4, fraction from 100 mM imidazole elution; Lanes, 5, 6, and 7, fractions from 250 mM imidazole elution. HydE appears at approximately 41,600 Da.

HydF Glycine to Alanine Mutations

Nine liter cultures of the $HydF^{\Delta EG}$ glycine residue 19 to alanine ($HydF(G19A)^{\Delta EG}$) mutant expressed in *E. coli* typically resulted in 30 to 35 grams of cells, with approximately 15 g used for a purification. A 15 g cell pellet for purification would result in approximately 40 mg of purified protein. Iron content ranged from 0.9 to 1 Fe/protein. The protein eluted from the column at 100 to 250 mM imidazole with an estimated purity of greater than 95% (Figure 3.6).

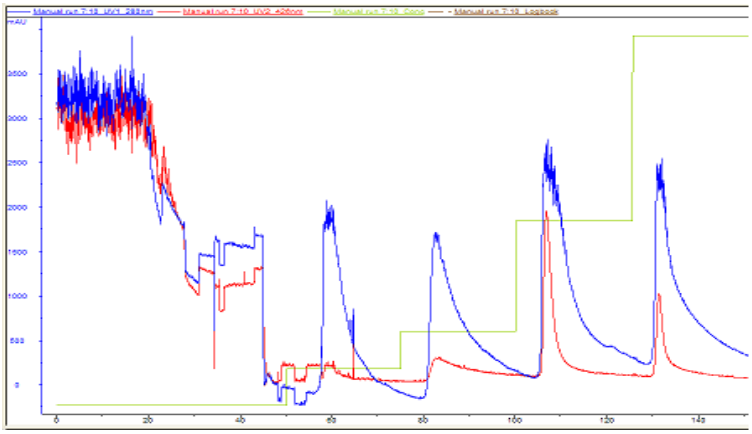

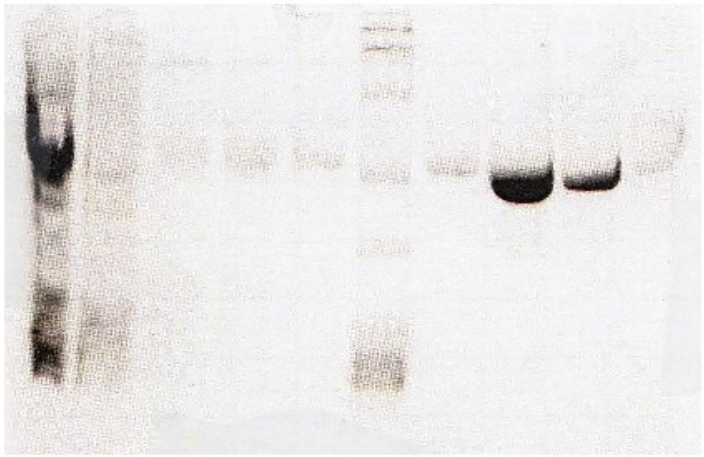

Figure 3.6 Purification of HydF(G19A)$^{\Delta EG}$. Chromatogram obtained upon purification of HydF(G19A)$^{\Delta EG}$ (top) and SDS-PAGE analysis of fractions obtained (bottom). On the chromatogram, the blue line represents A_{280}, the red line shows A_{426} for monitoring [Fe-S] clusters. Aliquots of fractions (15 µL each) were loaded in each lane. Lane 1, cell extract; Lane 2, flow through; Lanes 3, 4, and 5, fractions collected from the 100 mM imidazole elution; Lane 6, molecular weight marker; Lanes 7, 8, 9, and 10, fractions collected from the 250 mM imidazole elution.

Nine liter cultures of the HydF$^{\Delta EG}$ glycine residue 24 to alanine (HydF(G24A)$^{\Delta EG}$) mutant expressed in *E. coli* typically resulted in 30 to 35 grams of cells, with approximately 15 g used for a purification. A 30 g cell pellet was purified which resulted in approximately 100 mg of purified protein. Iron content was found to be

0.32 ± 0.02 Fe/protein. The protein eluted from the IMAC column at 100 to 500 mM imidazole and was estimated to be greater than 95% pure (Figure 3.7).

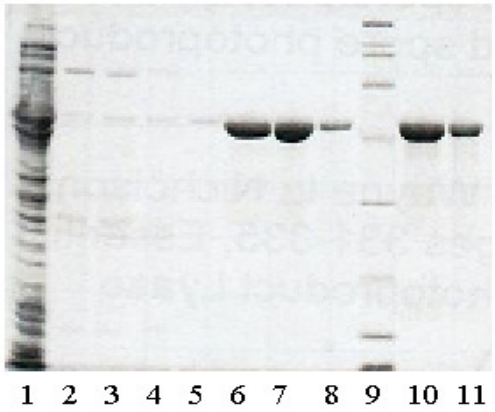

Figure 3.7 SDS-PAGE analysis of a HydF(G24A)$^{\Delta EG}$ mutant purification. Aliquots of fractions (10 µL each for lanes 1-4, 10 and 11, 7 µL each for lanes 5-9) were loaded in each lane. Lane 1, cell extract; Lanes 2, 3, and 4, fractions from 100 mM imidazole elution; Lanes 5, 6, 7, and 8, fractions from 250 mM imidazole elution; Lane 9 molecular weight marker; Lanes 10 and 11 from 500 mM imidazole elution.

HydF Serine to Alanine Mutations

Nine liter cultures of the HydF$^{\Delta EG}$ serine 26 to alanine (HydF(S26A)$^{\Delta EG}$) mutant expressed in *E. coli* typically resulted in 20 to 25 grams of cells, with approximately 10 g used for a purification. A 10 g cell pellet purification would result in approximately 40 mg of purified protein. Iron content was found to range from 0.2 to 0.4 Fe/protein. HydF(S26A)$^{\Delta EG}$ elutes from the IMAC column at 100 to 500 mM imidazole with a purity estimated at greater than 90% (Figure 3.8).

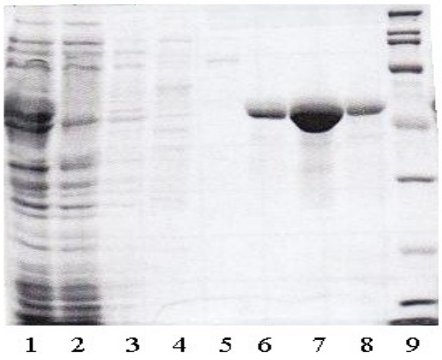

Figure 3.8 SDS-PAGE analysis of a HydF(S26A)$^{\Delta EG}$ mutant purification. Aliquots of fractions (10 µL each) were loaded in each lane. Lane 1, cell extract; Lane 2, flow through; Lane 3, wash; Lane 4, fraction from 50 mM imidazole elution; Lane 5, fraction from 100 mM imidazole elution; Lanes 6 and 7, fractions from 250 mM imidazole; Lane 8, fraction from 500 mM imidazole; Lane 9, molecular weight marker.

A 4.5 liter culture of the serine 26 to alanine (HydF(S26A)^{EG}) mutant expressed in *E. coli* resulted in 16.2 grams of cells, all of which were used for a purification. The purification resulted in approximately 25 mg of purified protein, with less than 0.01 Fe/protein; an iron assay was unable to detect iron in the protein. HydF(S26A)^{EG} elutes from the IMAC column at 100 to 250 mM imidazole with a purity estimated at greater than 90% (Figure 3.9).

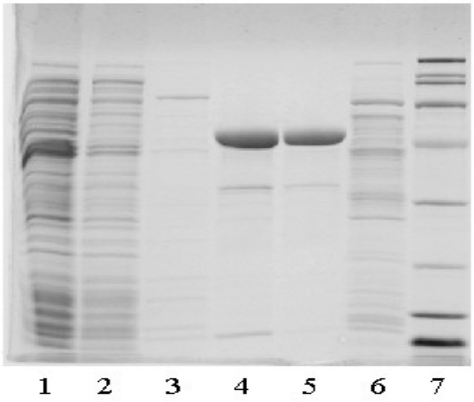

Figure 3.9 SDS-PAGE analysis of a HydF(S26A)^{EG} mutant purification. Aliquots of fractions (10 µL each for Lanes 1 and 2; 15 µL each for lanes 3-7) were loaded in each lane. Lane 1, cell extract; Lane 2, flow through; Lane 3 is a fraction collected during the 100 mM imidazole elution; Lanes 4 and 5 were collected during the 250 mM elution; Lane 6 was a sample taken from the 50 mM imidazole wash; Lane 7, molecular weight marker.

HydF Cysteine to Serine Mutation

A 9 liter culture of the HydF(C353S)^{EG} mutant expressed in *E. coli* typically resulted in 20 to 25 grams of cells, with approximately 10 g used for a purification. A 10 g cell pellet purification would result in approximately 40 mg of purified protein, with a range of 0.3 to 1.4 Fe/protein. HydF(C353S)^{EG} eluted from the IMAC column at 100 to 500 mM imidazole with a purity of ~90% (Figure 3.10).

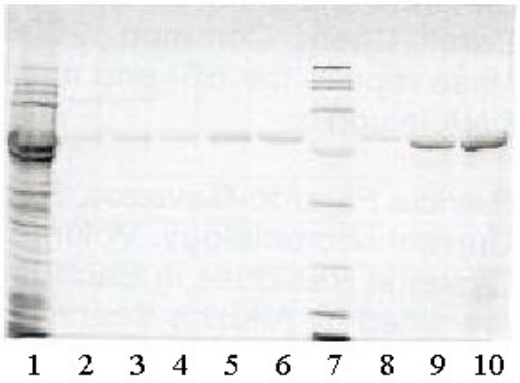

Figure 3.10 SDS-PAGE analysis of a HydF$^{\Delta EG}$ C353S mutant purification. 20µL of each sample was loaded in Lanes 1 and 10; 12 µL of each sample was loaded in lanes 2-9. Lane 1, supernatant; Lanes 2-5 were collected during the 100 mM imidazole elution; Lane 6, fraction from the 250 mM elution; Lane 7, molecular weight marker; Lanes 8-10 were collected from fractions of the 500 mM imidazole elution.

Generation of Iron-Depleted and Reconstituted HydF

HydF$^{\Delta EG}$ stripped of the iron-sulfur cluster, and with reconstituted cluster was examined by UV-Vis spectroscopy to determine if an [Fe-S] cluster was present. This confirmed no iron presence in the apo-protein, and a $[4Fe4S]^{2+}$ cluster in the reconstituted protein (Figure 3.11).

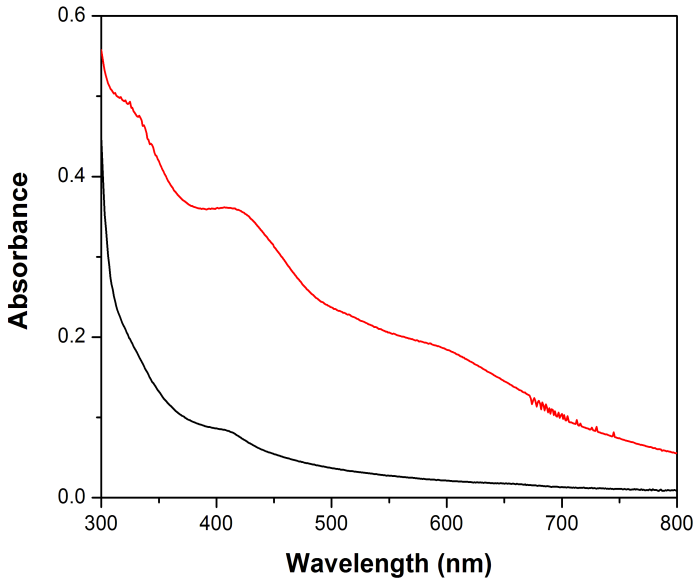

Figure 3.11 UV-visible spectra of iron-depleted and reconstituted $HydF^{\Delta EG}$. $HydF^{\Delta EG}$ stripped (~160 µM, black) and $HydF^{\Delta EG}$ reconstituted (~60 µM, red).

GTPase Assays

The hydrolysis of GTP to GDP by HydF was assayed by incubating HydF with 2 mM each $MgCl_2$, DTT, and GTP, quenching the reaction at a specific time point with HCl, and then monitoring for the presence of GTP and GDP by HPLC. On the reverse phase C18, 4.6 x 150 mm column, GDP elutes first at approximately 5 minutes, and GTP elutes second at approximately 8 minutes. Figure 3.12 shows a typical chromatogram obtained upon HPLC analysis of an assay that demonstrates changes in presence of GDP and GTP over time. For each set of assays, controls were made and a $HydF^{EG}$ GTPase assay was performed to ensure the activity of the enzyme. Multiple GTPase assays were performed with $HydF^{EG}$ to ensure consistent results among assays (Figure 3.13).

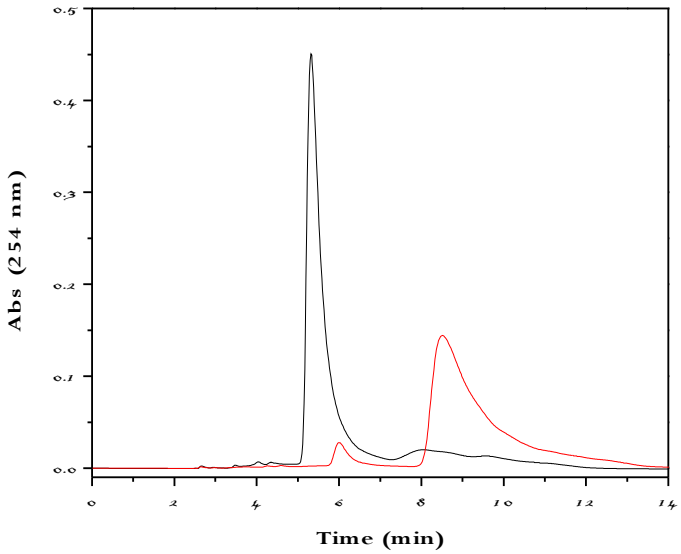

Figure 3.12 Representative HPLC Chromatograms used to quantify GTPase activity. Under the conditions used, GDP elutes at 5 min and the GTP elutes at 7.5 min. Control assay (red) compared to one performed with active protein ($HydF^{\Delta EG}$ S26A, black) at 16 minutes. HydFΔEG S26A (70 µM) was incubated at 30°C in 50 mM HEPES, 0.5 M KCl, 5% glycerol, pH 7.4 buffer, with 2 mM $MgCl_2$, 2 mM DTT, and 2 mM GTP.

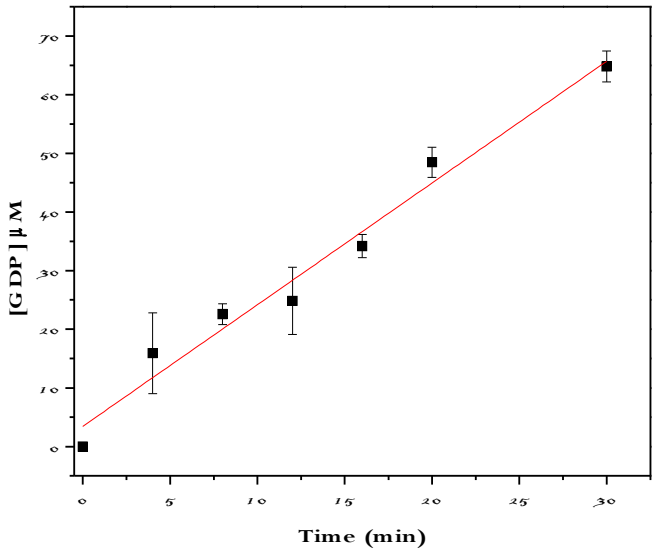

Figure 3.13 Plot of integrated intensities of the GDP peak versus time from HPLC chromatograms for $HydF^{EG}$. Two data points were taken at each time point. The assay was performed at 30°C in 50 mM HEPES, 0.5 M KCl, 5% glycerol, pH 7.4, with 2mM DTT, 2mM $MgCl_2$, 2mM GTP, and 1 µM $HydF^{EG}$.

Effects of Cluster Content

The GTP hydrolysis rates of $HydF^{\Delta EG}$ after stripping and reconstitution were measured and compared to determine what effect, if any, the [Fe-S] content of the enzyme had on GTPase activity. The concentration of GDP at each time point was determined and graphed versus time, as illustrated in Figures 3.14 and 3.15. The data was analyzed via linear regression, and the slope was used to determine k_{cat} (Table 1).

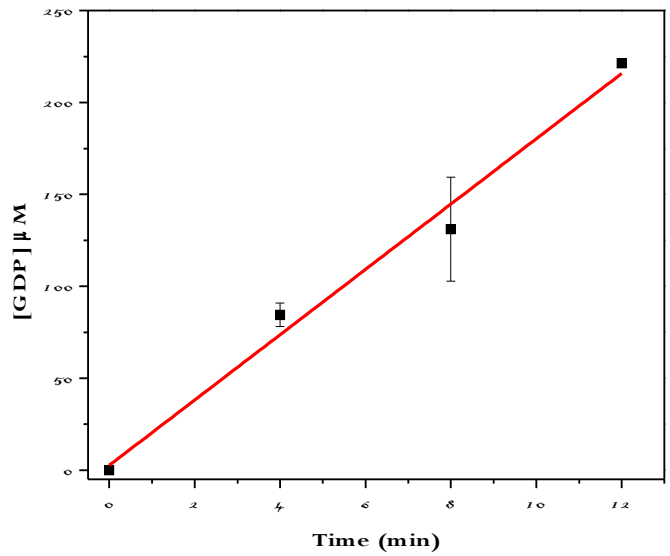

Figure 3.14 Plot of integrated intensities of the GDP peak versus time from HPLC chromatograms for $HydF^{\Delta EG}$ stripped of Fe. Two data points were taken at each time point. The assay was performed at 30°C in 50 mM HEPES, 0.5 M KCl, 5% glycerol, pH 7.4, with 2 mM DTT, 2 mM $MgCl_2$, 2 mM GTP, and 7 µM $HydF^{\Delta EG}$.

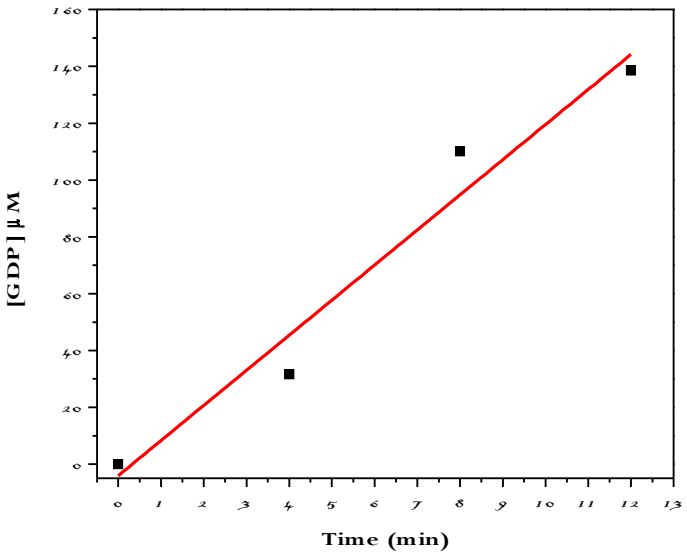

Figure 3.15 Plot of integrated intensities of the GDP peak versus time from HPLC chromatograms for $HydF^{\Delta EG}$ reconstituted. One data point was taken at each time point. The assay was performed at 30°C in 50 mM HEPES, 0.5 M KCl, 5% glycerol, pH 7.4, with 2 mM DTT, 2 mM $MgCl_2$, 2 mM GTP, and 7 μM $HydF^{\Delta EG}$.

The k_{cat} for GTP hydrolysis for $HydF^{\Delta EG}$ stripped of Fe was 2.5 ± 0.3 min^{-1}, and for $HydF^{\Delta EG}$ reconstituted with [Fe-S] was 1.8 ± 0.2 min^{-1}. The k_{cat} for $HydF^{EG}$ is within error of the turnover rate for the bot the stripped and reconstituted protein (2.1 ± 0.4 min^{-1} for $HydF^{EG}$), indicating that iron or [Fe-S] clusters do not play a significant role in GTP hydrolysis.

Effects of Accessory and Structural Hyd Proteins

To investigate the possibility of GTP hydrolysis being involved in the transfer of [Fe-S] cluster or ligands between the other accessory proteins, HydE and HydG, and the structural protein HydA, assays were performed individually with $HydF^{EG}$ in the presence

of $HydG^{EF}$, $HydE^{FG}$, or $HydA^{\Delta EFG}$. Changes in rates of GTP hydrolysis in the presence of these other proteins could be interpreted as evidence for a role for GTP hydrolysis in the interactions between HydF and the other proteins. As can be seen in Table 1 and in Figures 3.16, 3.17, and 3.18 show the specific plots for each assay.

Table 1
Catalytic Activity for $HydF^{EG}$ in the presence of Structural and Accessory Proteins

Protein	HydF: Protein	Activity min^{-1}
$HydF^{EG}$	NA	2.06 ± 0.42
$HydA^{\Delta EFG}$	1:10	2.2 ± 0.37
$HydG^{EF}$	1:10	3.44 ± 0.68
$HydE^{FG}$	1:10	3.03 ± 0.36

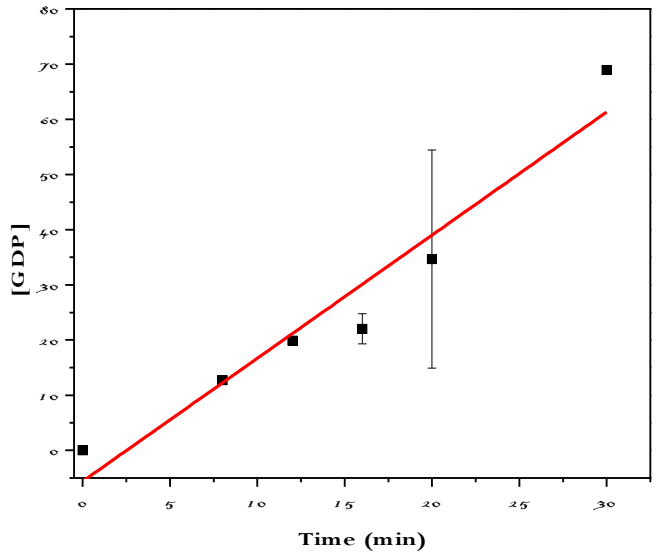

Figure 3.16 Plot of integrated intensities of the GDP peak versus time from HPLC chromatograms for $HydF^{\Delta EG}$ (1μM) in the presence of $HydA^{\Delta EFG}$ (10 μM). One or two data points were taken at each time point. The assay was performed at 30°C in 50 mM HEPES, 0.5 M KCl, 5% glycerol, pH 7.4, with 2m M DTT, 2 mM $MgCl_2$, and 2 mM GTP.

$HydF^{EG}$ in the presence of $HydA^{\Delta EFG}$ has a k_{cat} (2.2 ± 0.4 min^{-1}) comparable to that of $HydF^{EG}$ alone ($2.1 \pm 0.4 min^{-1}$), suggesting that GTP hydrolysis is not associated with any subcluster transfer to the hydrogenase. The data presented for HydF in the presence of HydA is preliminary, and at this time serves to give some idea of how HydA may affect GTPase activity. $HydF^{EG}$ in the presence of both $HydE^{FG}$ and $HydG^{EF}$ shows an increase in the rate of GTP hydrolysis (3.03 ± 0.36 min^{-1} and 3.44 ± 0.68 min^{-1}, respectively, compared to 2.06 ± 0.42 min^{-1} for $HydF^{EG}$ alone), suggesting a possible cluster or ligand transfer from $HydG^{EF}$ and or $HydE^{FG}$ to $HydF^{EG}$ associated with GTP hydrolysis. The transfer of cluster or cluster components to HydF supports our hypothesis that $HydF^{EG}$ acts as a scaffold.

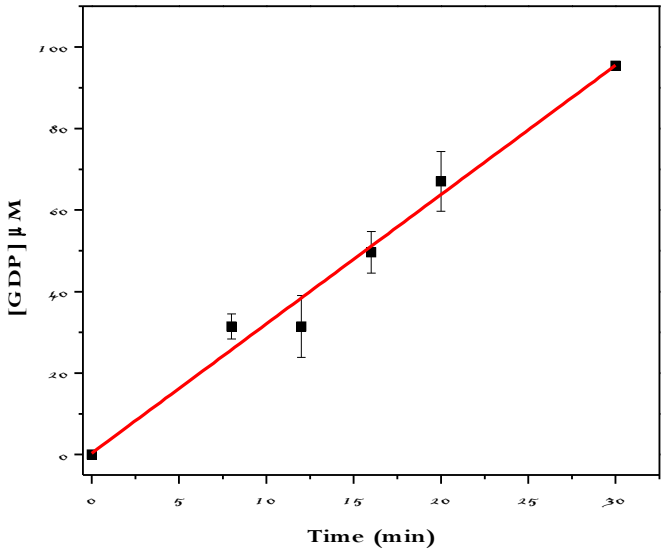

Figure 3.17 Plot of integrated intensities of the GDP peak versus time from HPLC chromatograms for $HydF^{\Delta EG}$ (1 μM) in the presence of $HydG^{EF}$ (10 μM). Two data points were taken at each time point. The assay was performed at 30°C in 50 mM HEPES, 0.5 M KCl, 5% glycerol, pH 7.4, with 2 mM DTT, 2 mM $MgCl_2$, and 2 mM GTP.

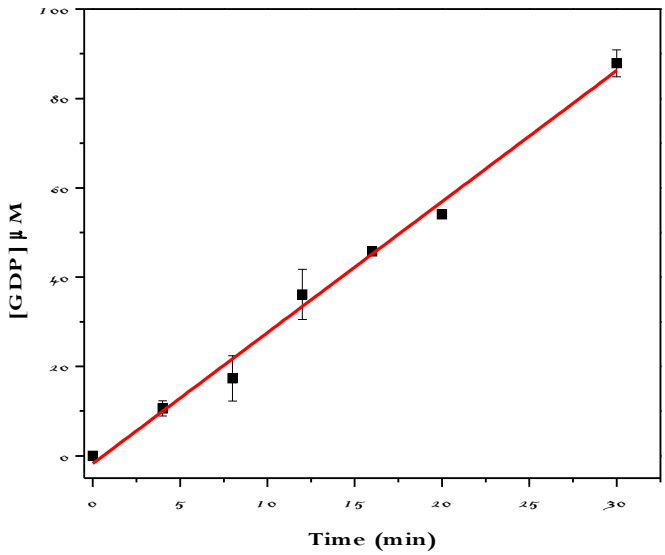

Figure 3.18 Plot of integrated intensities of GDP peak versus time from HPLC chromatograms for Hyd F^{EG} (1µM) in the presence of $HydE^{FG}$ (10 µM). Two data points were taken at each time point. The assay was performed at 30°C in 50 mM HEPES, 0.5 M KCl, 5% glycerol, pH 7.4, with 2 mM DTT, 2 mM $MgCl_2$, and 2 mM GTP.

Role of Specific HydF Residues

Four mutants of HydF sequence were evaluated for their effect on HydF GTPase activity. It was shown previously that these same HydF mutants coexpressed with HydE, HydG, and HydA resulted in the inability of the coexpressed enzymes to produce hydrogen (37). Three of the residues examined, the G19, G24, and S26 residues, are found in the conserved P-loop GxxxxGK(S/T) motif involved in GTP coordination (47). The HydF variants G19A and G24A exhibited significantly decreased GTPase activity

(Table 2). This observation supports the central role of these residues in binding GTP for hydrolysis.

The third P-loop variant, HydF(S26A), retains GTPase activity (2.2 ± 0.4 min^{-1} for $HydF^{\Delta EG}$, and 1.9 ± 0.2 min^{-1} for $HydF^{EG}$), near that of the wild type (2.0 ± 0.3 min^{-1} for $HydF^{EG}$), seen in Figures 3.19 and 3.20. This retention of GTPase activity was surprising, given that this same variant resulted in a complete loss of hydrogen evolution in whole cell extracts from *E. coli* (37). Our results demonstrate that while HydF serine 26 plays a critical role in hydrogenase maturation, it is not critical to the GTPase activity of HydF, despite being located in the conserved Walker P-loop.

Figure 3.21 compares UV-visible spectra of the HydF S26A variant in two different backgrounds, from $HydF^{EG}$ and $HydF^{\Delta EG}$. The shoulders seen at 410 nm and possibly at 590 nm in the $HydF^{\Delta EG}$ spectra are characteristic of $[4Fe\text{-}4S]^{2+}$ and $[2Fe\text{-}2S]^{2+}$ clusters. The $HydF^{EG}$ mutant appears to lack iron-sulfur cluster content, which corresponds with the inability to detect iron in an iron assay. This may explain why the mutation in whole cell extracts was unable to activate HydA, if there was no cluster to transfer or modify, and suggests the conserved serine plays a role in binding iron. It is important to note the experiments carried out here with the $HydF^{EG}$ S26A enzyme came from one purification and need further confirmation.

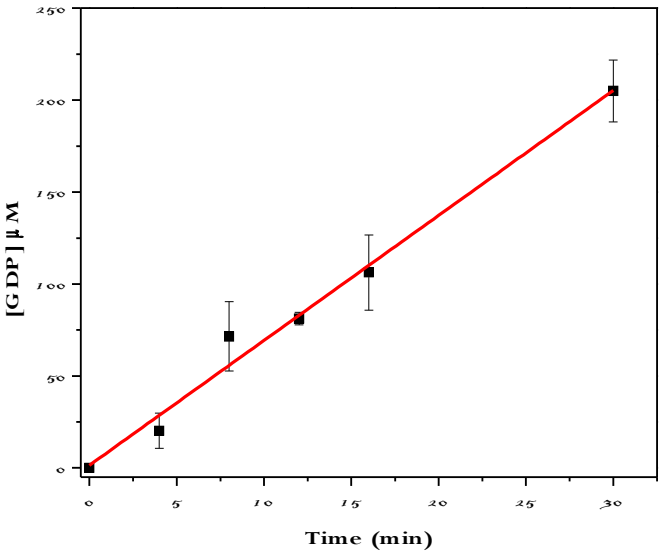

Figure 3.19 Plot of integrated intensities of the GDP peak versus time from HPLC chromatograms for HydF(S26A)$^{\Delta EG}$ (4 µM). Two data points were taken at each time point. The assay was performed at 30°C in 50 mM HEPES, 0.5 M KCl, 5% glycerol, pH 7.4, with 2mM DTT, 2mM $MgCl_2$, and 2mM GTP.

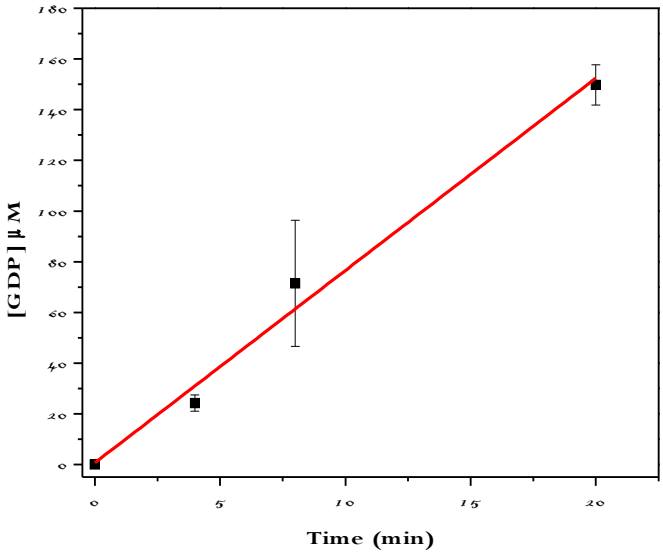

Figure 3.20 Plot of integrated intensities of the GDP peak versus time from HPLC chromatograms for HydF(S26A)^{EG} (4 µM). Two data points were taken at each time point. The assay was performed at 30°C in 50 mM HEPES, 0.5 M KCl, 5% glycerol, pH 7.4, with 2 mM DTT, 2 mM $MgCl_2$, and 2 mM GTP.

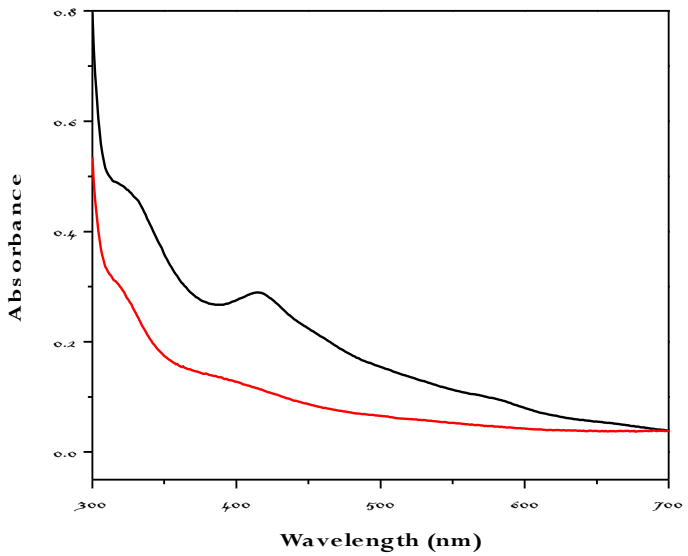

Figure 3.21 Normalized chromatogram of HydF(S26A)^{EG} compared to HydF(S26A)$^{\Delta EG}$. HydF(S26A)^{EG} shown in red, HydF(S26A)$^{\Delta EG}$ shown in black. Both enzymes are shown at 280 µM, in 50 mM HEPES, 0.5 M KCl, 5% glycerol, pH 7.4.

The fourth HydF variant studied was a HydF Cys353Ala; Cys353 is one of three cysteines found in the *C. acetobutylicum* HydF sequence that may be involved in [Fe-S] cluster ligation. The HydF C353S mutant showed dramatically decreased GTPase activity as well (Figure 3.22). This result is somewhat surprising, as few GTPases bind metal clusters (40), and thus the [Fe-S] cluster is not expected to be directly involved in GTP hydrolysis. The loss of GTPase activity may point to a larger role for the mutated residue or for the [Fe-S] cluster itself. For example, if the iron-sulfur cluster were involved in protein dimerization. HypB, the nickel transporting protein of [Ni-Fe] hydrogenase, and the salt ion dependent MnmE GTPases both form dimers(44)(45). It is possible then that the cysteine residue or [Fe-S] cluster it binds could be involved in protein dimerization necessary to properly build a cluster precursor on HydF.

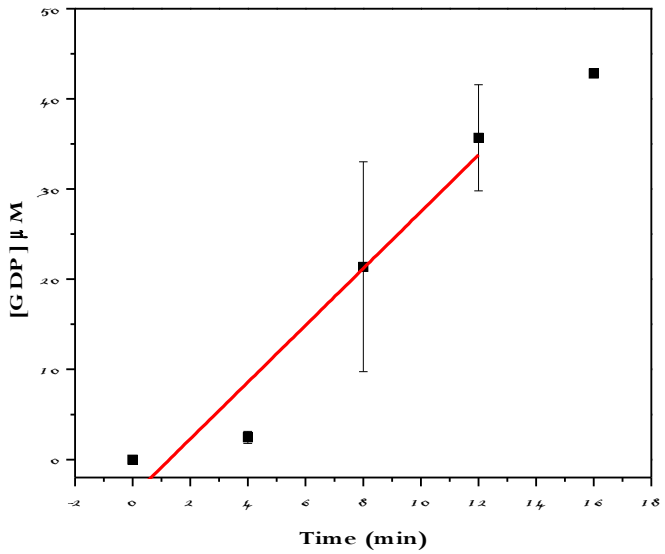

Figure 3.22 Plot of integrated intensities of the GDP peak versus time from HPLC chromatograms for HydF(C353S)$^{\Delta EG}$ (70 µM). Two data points were taken at each time point. The assay was performed at 30°C in 50 mM HEPES, 0.5 M KCl, 5% glycerol, pH 7.4, with 2 mM DTT, 2 mM $MgCl_2$, 2 mM GTP.

Table 2 Catalytic Activity for HydF Mutations

Background	Mutation	Iron number/Protein	Activity min^{-1}
HydF$^{\Delta EG}$	G19A	0.89 - 1.04	0.01 ± 0.01
HydF$^{\Delta EG}$	G24A	0.32	0.03 ± 0.01
HydF$^{\Delta EG}$	S26A	0.23 - 0.43	2.22 ± 0.41
HydF^{EG}	S26A	<0.01	1.89 ± 0.23
HydF$^{\Delta EG}$	C353S	0.28 - 1.4	0.04 ± 0.01

DISCUSSION

Effects of Metal Cluster Content

The k_{cat} determined for HydF depleted of its iron-sulfur cluster (2.5 ±0.3 min^{-1}) and with reconstituted [Fe-S] cluster (1.8 ± 0.2min^{-1}) are within error of that for the wild type protein (2.1 ± 0.4 min^{-1}), showing GTPase activity of HydF does not depend on iron content. This confirms initial observations made by Brazzolotto *et al.* with the *Thermotoga maritima* HydF (40). If GTP hydrolysis occurs independently of a metal cluster, then the [Fe-S] cluster is likely required elsewhere in the HydA maturation process. Recent results have shown HydA grown in the absence of HydE, HydF, and HydG ($HydA^{\Delta EFG}$) contains the [4Fe-4S] cluster of the active site, but lacks the [2Fe-2S] subcluster necessary for hydrogenase activity (32). HydF, already shown to be a scaffold (30), may be providing the [Fe-S] cluster as a scaffold site for addition of either more iron and sulfur atoms, or nonprotein CO, CN^-, and dithiolate ligands, or all of the above for eventual transfer to $HydA^{\Delta EFG}$.

Effect of other Hyd Proteins on GTPase Activity

Although results to date are preliminary, the GTPase assay of $HydF^{EG}$ in the presence of $HydA^{\Delta EFG}$ indicates the hydrogenase structural protein does not influence HydF GTPase activity. $HydF^{EG}$ alone hydrolyzed GTP at 2.06 ± 0.42 min^{-1} compared to $HydF^{EG}$ in the presence of $HydA^{\Delta EFG}$ at 2.2 ±0.37 min^{-1}. This important result compliments a previous observation that the presence of GTP is not a requirement for

activation of hydrogenase by "loaded" $HydF^{EG}$ (30). Further sample analysis will help confirm these results.

In the presence of either HydE or HydG, the GTPase activity of HydF increases by approximately 50%, indicating a change may take place upon the interaction of the proteins that favors the hydrolysis of GTP. The increase in activity also indicates GTP hydrolysis could be involved in cluster formation on the scaffold or transfer of a cluster precursor to the scaffold. HydF and HydE working in concert is not too surprising, considering the proteins were initially found as one multidomain protein in *C. reinhardtii* (5). Based on previously established ideas of HydF acting as scaffold (30), HydE performing a role as sulfur donor (34), and HydG contributing nonprotein ligands through the breakdown of the cleavage products of tyrosine, an outline of hydrogenase maturation begins to form, in which increased GTPase activity in the presence of the other two accessory proteins may provide a mechanism for cluster assembly. Much of this process must be experimentally demonstrated, and many questions need to be answered regarding specific protein interactions and the mechanism of formation of small molecules.

Role of Specific HydF Amino Acid Residues in GTP Hydrolysis

The near complete loss of GTPase activity observed with two mutations in the Walker A P-loop (G19 and G24) indicates that these mutated residues are essential to GTP hydrolysis, not merely for optimization of the active site. Glycine residues located in the Walker A P loop are known to allow tight angles not achievable with other amino

acids (48). These angles allow up to four amides of amino acids in the P loop to hydrogen bond with the α and β phosphate groups of GTP (49). Mutations of two of the conserved glycine residues (G19 and G24) in the Walker A P loop results in nearly no activity (0.01 ± 0.01 min^{-1} for G19A and 0.03 ± 0.01 min^{-1} for G24A). This data suggests that the mutated P-loop has a dramatically decreased ability to coordinate GTP, likely due to the inability to form key hydrogen bonds to the phosphate groups of GTP. These mutations also correspond to a significant decrease in hydrogen evolving activity by HydA in whole cell extracts of *E. coli* (37).

The loss of GTPase activity reflects a change in proper substrate binding by the HydF mutants, while loss of H_2 evolution by $HydA^{\Delta EFG}$ in whole cell extracts may reflect altered interactions of HydF with HydE and HydG as a result of the inability to properly bind and hydrolyze GTP or structural changes in the P loop that interfere with protein interactions. HydF would then lack the necessary component(s) to activate HydA.

The HydF S26A mutation, also in the P-loop, was associated with a lack of hydrogen reduction in whole *E. coli* cells. Unlike the other mutations, however, the S26A variant does hydrolyze GTP. In this case the serine must not play as significant a role as the glycines do in binding GTP. Typically the serine coordinates the Mg^{2+} essential to GTPase activity (49), but in the case of MnmE other residues and small molecules also take part in binding the magnesium ion, including a β-phosphate oxygen from GTP, a conserved threonine, and a water molecule (45). In the case of HypB (the metal delivery protein for [NiFe]-hydrogenase) a threonine found in the P-loop motif binds the magnesium ion (44). Figure 4.1 shows the nucleotide binding interactions of

HypB, which dimerizes upon coordination of GTP. Including the threonine of HypB, the amino acids that are involved in binding the Mg^{2+} all have oxygen atoms coordinated to the magnesium ion. Figure 4.2 shows MnmE, which coordinates a serine to the magnesium ion, highlighted by a yellow box.

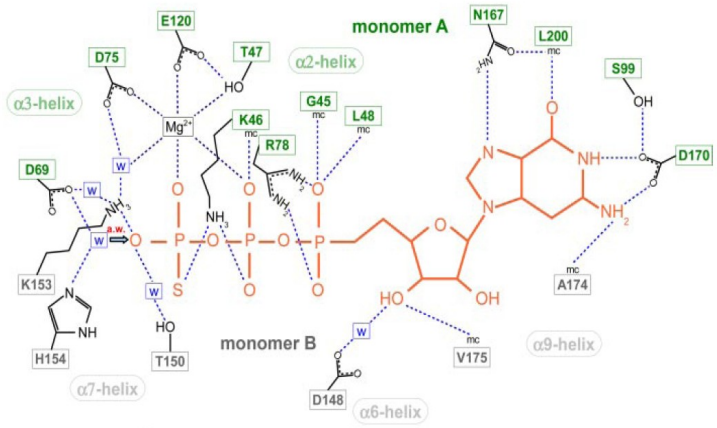

Figure 4.1 GTP binding by HypB from *M. jannaschii* showing Mg^{2+} and GTP coordination (44).

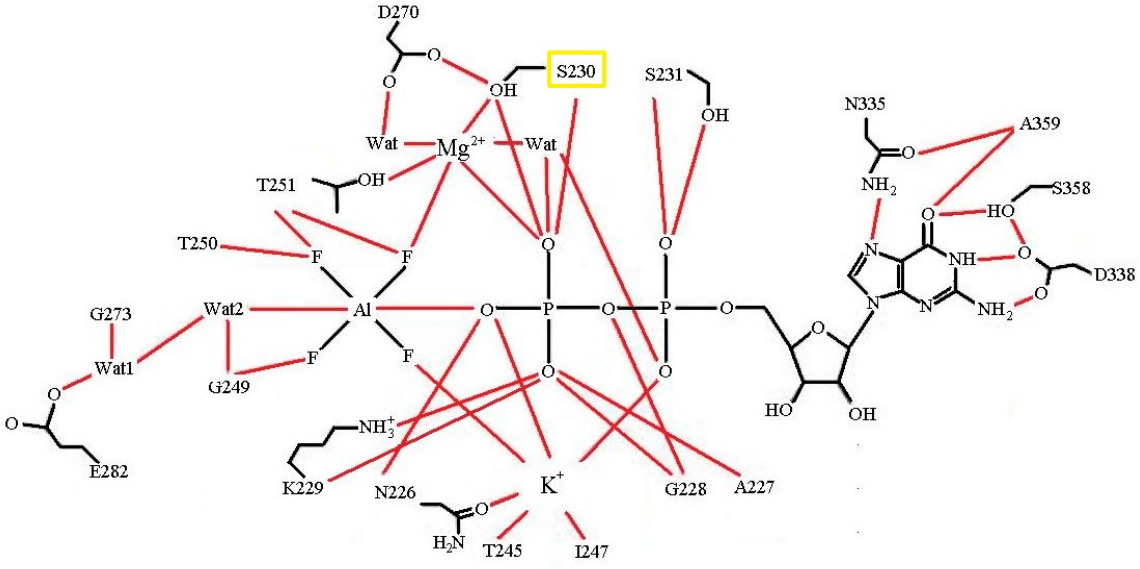

Figure 4.2 GTP binding by MnmE from *E. coli*, showing Mg^{2+} and GDP-AlF_4^- coordination, revised from Scrima *et al* .(45).

In the P loop motif, GxxxxGKS/T, the last amino acid can be a serine or a threonine, and mutations from serine to threonine have demonstrated little change in

nucleotide binding affinity (50). Mutations of the conserved serine have been studied in H-Ras, a GTP-binding protein involved in cell growth and in adenylate cyclase regulation (51). Mutation to glycine or threonine appears to have only a small affect on GTP binding affinity. In the case of the threonine an oxygen interaction with the Mg^{2+} is maintained. It is postulated the glycine mutation results in such a small side group that a water molecule is able to fit in the remaining space to coordinate the magnesium ion. Serine to cysteine, alanine, and asparagine mutations were also studied, and appeared to have 20-fold greater affinity for binding GDP than GTP (51). Native GTP binding ability was not returned upon addition of Mg^{2+}, and the addition of a chelating agent (EDTA) to wild-type H-Ras did not result in a decreased affinity for GTP (51). This indicated the change in binding affinity did not result from a loss of ability to coordinate magnesium, but rather from the improper coordination of magnesium. In the case of the $HydF^{EG}$ and $HydF(S26A)^{\Delta EG}$ mutation, the activity is essentially the same as that of wild type HydF (1.89 ± 0.23 min^{-1} and 2.22 ± 0.41 min^{-1} for $HydF(S26A)^{EG}$ and $HydF(S26A)^{\Delta EG}$ respectively, compared to 2.05 ± 0.26 min^{-1} for $HydF^{EG}$), indicating the magnesium ion is bound by other components in HydF. However, the result that the S26A mutant is unable to mature $HydA^{\Delta EFG}$ suggests that the serine residue in HydF may have dual roles in coordinating Mg^{2+} and/or is involved in key protein-protein interactions which result in proper cluster assembly on HydF. Further study of the interaction of this HydF variant in the presence of HydE, HydG, and HydA would yield interesting insight into the reaction mechanism.

UV-Visible spectroscopy indicates that very little iron is bound by the serine mutated HydF grown in the background of HydE and HydG, but the HydF S26A grown in the absence of these proteins binds significantly more iron. The absence of an [Fe-S] cluster on $HydF^{EG}$ S26A may explain why the mutation in whole cell extracts was unable to activate HydA if there was no cluster to transfer or modify, and suggests the conserved serine plays a role in binding iron. This would be an unprecedented result which requires further experimental testing.

The ability of the S26A variant to hydrolyze GTP, together with its inability to activate HydA lends credence to previous suggestions that GTP hydrolysis is not tied to cluster transfer from HydF to HydA. In addition, these results suggest the presence of two active sites for HydF, one for GTPase activity and one that acts as a scaffold for an [Fe-S] cluster.

The HydF C353S variant results in loss of GTPase activity of HydF (0.04 ± 0.01 min^{-1}). It was anticipated that the cysteine residue would be involved in binding the [Fe-S] cluster of the enzyme because it is one of three conserved cysteine residues found in the HydF sequence from *C. acetobutylicum*. Results from stripping HydF of metal still yield an active GTPase, so the removal of a ligand thought to bind the [Fe-S] cluster was expected to have the same effect as no metal bound: no loss of activity. This changed residue resulting in loss of activity must have a function outside of binding iron, which could include a role in protein dimerization.

CONCLUSION

Many advances in understanding active site assembly of the [Fe-Fe]-hydrogenase have been made since the structure was first published ten years ago (52), yet several questions remain. Initial identification of HydF indicated it was a GTPase, but what (if any) role GTP hydrolysis played in maturation of HydA was unclear. Our findings that HydE and HydG facilitate GTPase activity along with evidence that mutations previously shown cease hydrogenase activity (37) also drastically reduce HydF GTPase activity indicate an important role for GTP hydrolysis in hydrogenase maturation. The HydF mutation that retains activity, S26A, shows loss of hydrogenase activity in whole cell extracts that could result from disrupted magnesium binding, which may in turn affect conformation or binding environments of HydF that would disrupt a number of potential HydF interactions: HydE and HydG binding, insertion of ligands onto a scaffold, cluster transfer to HydA, or binding with HydA. The C353S mutation may also play a role in the structure, scaffolding, or cluster transfer ability of HydF, as its anticipated role binding an [Fe-S] cluster should not hinder GTPase activity, as demonstrated by GTPase activity in the apo-protein.

Structural determination of HydF is essential to understanding the functional roles of HydF. Barring that, investigation of ligands for the iron-sulfur cluster could shed light on the iron-sulfur cluster properties. Preliminary research has indicated HydF is a dimer (manuscript in preparation), and identification of cluster ligands could elucidate roles of

specific residues in cluster or protein binding. An assay of HydF GTPase activity with both HydE and HydG present would clarify the interactions of the three proteins.

REFERENCES CITED

(1) Adams, M. W. W.; Stiefel, E. I.. Biological Hydrogen Production: Not So Elementary. *Science*, **1998,** *282*, 1842-1843.

(2) Cammack, R., *Hydrogenase in biotechnology: Hydrogen consumption,* Taylor & Francis: London, 2001; 181-200.

(3) Vignais, P.M.; Billoud, B.; Meyer, J. Classification and phylogeny of hydrogenases. *FEMS Microbiol. Rev.,* **2001,** *25,* 455-501.

(4) Fontecilla-Camps, J. C.; Volbeda, A.; Cavazza, C.; Nicolet, Y. Structure/Function Relationships of [NiFe]- and [FeFe]-Hydrogenases. *Chem. Rev.,* **2007,** *107,* 4273-4303.

(5) Posewitz, M. C.; King, P. W.; Smolinski, S. L.; Zhang, L.; Seibert, M.; Ghirardi, M. L.. Discovery of Two Novel Radical S-Adenosylmethionine Proteins Required for the Assembly of an Active [Fe] Hydrogenase. *The Journal of Biological Chemistry*, **2004,** *279*, 25711-25720.

(6) Beinert, H.; Holm, R.H.; Munck, E. Iron-Sulfur Clusters: Nature's Modular, Multipurpose Structures. *Sci.* **1997,** *277,* 653-659.

(7) Malkin, R.; Rabinowitz, J. C.. The reconstitution of *clostridial* ferredoxin. *Biochem. Bioph. Res. Co.* **1966,** *23,* 822-827.

(8) Johnson, D.C.; Dean, D.R.; Smith, A.D.; Johnson, M.K.; Structure, Function, and Formation of Biological Iron-Sulfur Clusters. *Annu. Rev. Biochem.,* **2005,** *74,* 247-281.

(9) Plaxco, K. W.; Gross, M., *Astrobiology: A Brief Introduction,* Johns Hopkins University Press: Baltimore, 2006; 92-116.

(10) Russel, M. J. The Alkaline Solution to the Emergence of Life: Energy, Entropy, and Early Evolution. *Acta Biotheor.,* **2007,** *55,* 133-179.

(11) Howard, J. B.; Rees, D. C.. Structural Basis of Biological Nitrogen Fixation. *Chemical Reviews*, **1996,** *96*, 2965-2982.

(12) Grandoni, J.A.; Switzer, R.L.; Makaroff; C.A.; Zalkin, H. Evidence That the Iron-Sulfur Cluster of *Bacillus subtilis* Glutamine Phosphoribosylpyrophosphate Amidotransferase Determines Stability of the Enzyme to Degradation *in vivo*. *J. Biol. Chem.,* **1989,** *264,* 6058-6064.

(13) Sofia, H. J.; Chen, G.; Hetzler, B. G.; Reyes-Spindola, J. F.; Miller, N. E.. Radical SAM, a novel protein superfamily linking unresolved steps in familiar biosynthetic pathways with radical mechanisms: functional characterization using new analysis and information visualization methods. *Nucleic Acids Research*, **2001,** *29*, 1097-1106.

(14) Lazazzera, B. A.; Beinert, H.; Khoroshilova, N.; Kennedy, M. C.; Kiley, P. J. DNA Binding and Dimerization of the Fe-S-containing FNR Protein from Escherichia coli Are Regulated by Oxygen. *J. Biol. Chem.*, **1996,** *271*, 2762-2768.

(15) Volbeda, A.; Garcin, E.; Piras, C.; De Lacey, A. L.; Fernandes, V. M.; Hatchikian, E. C.; Frey, M.; Fontecilla-Camps, J. C. Structure of the [NiFe] hydrogenase active site: Evidence for biologically uncommon Fe ligands. *J. Am. Chem. Soc.,* **1996,** *118,* 12989-12996.

(16) Higuchi, Y.; Yagi, T.; Yasuoka, N. *Structure,* **1997,** *5,* 1671.

(17) Matias, P. M.; Soares, C. M.; Saraiva, L. M.; Coelho, R.; Morais, J.; Le Gall, J.; Carrondo, M. A. *J. Biol. Inorg. Chem.,* **2001,** *6,* 63.

(18) Ogata, H.; Hirota, S.; Nakahara, A.; Komori, H.; Shibata, N.; Kato, T.; Kano, K.; Higuchi, Y. *Structure,* **2005,** *13,* 1635.

(19) Volbeda, A.; Martin, L.; Cavazza, C.; Matho, M.; Faber, B. W.; Roseboom, W.; Albract, S. P.; Garcin, E.; Rousset, M.; Fontecilla-Camps, J. C. *J. Biol. Inorg. Chem.,* **2005,** *10,* 239.

(20) Posewitz, M. C.; Mulder, D. M.; Peters, J. W.. New Frontiers in Hydrogenase Structure and Biosynthesis. *Curr. Chem. Biol.,* **2008,** *2,* 178-199.

(21) Paschos, A.; Glass, R. S.; Bock, A.. Carbamoylphosphate requirement for synthesis of the active center of [NiFe]-hydrogenase. *FEBS Lett.,* **2001,** 488, 9-12.

(22) Blokesch, M.; Albracht, S. P. J.; Matzanke, B. F.; Drapal, N. M.; Jacobi, A.; Bock, A.. The complex Between Hydrogenase-maturation Proteins HypC and HypD is an Intermediate in the Supply of Cyanide to the Active Site Iron of [NiFe]-Hydrogenases. *J. Mol. Biol.,* **2004,** *344,* 155-167.

(23) Pandey, A. S.; Harris, T. V.; Giles, L. J.; Peters, J. W.; Szilagyi, R. K.. Dithiomethylether as a Ligand in the Hydrogenase H-Cluster. *J. Am. Chem. Soc.*, **2008,** *130*, 4533-4540.

(24) Nicolet, Y.; Piras, C.; Legrand, P.; Hatchikian, C. E.; Fontecilla-Camps, J. C. *Desulfovibrio desulfuricans* iron hydrogenase: the structure shows unusual coordination to an active site Fe binuclear center. *Structure*, **1999,** *7*, 13-23.

(25) Peters, J. W.. Structure and mechanism of iron-only hydrogenases. *Curr. Opin. Struct. Biol.,* **1999,** *9*, 670-676.

(26) Nicolet, Y.; de Lacey, A. L.; Vernde, X., Fernandez, V. M.; Hatchikian, C.; Fontecilla-Camps, J. C.. Crystallographic and FTIR Spectroscopic Evidence of Changes in Fe Coordination Upon Reduction of the Active Site of the Fe-Only Hydrogenase from *Desulfovibrio desulfuricans*. *J. Am. Chem. Soc.*, **2001,** *123*, 1596-1601.

(27) Zhou, T.; Mo, Y.; Liu, A.; Zhou, Z.; Tsai, K. R.. Enzymatic Mechanism of Fe-Only Hydrogenase: Density Functional Study on H-H Making/Breaking at the Diiron Cluster with Concerted Proton and Electron Transfers. *Inorg. Chem.*, **2004,** *43*, 923-930.

(28) Lemon, B. J.; Peters, J. W.. Binding of Exogenously Added Carbon Monoxide at the active Site of the Iron-Only Hydrogenase (CpI) from *Clostridium pasteurianum*. *Biochemistry*, **1999,** *38*, 12969-12973.

(29) McGlynn, S. E.; Ruebush, S. S.; Naumov, A.; Nagy, L. E.; Dubini, A.; King, P. W.; Broderick, J. B.; Posewitz, M. C.; Peters, J. W.. In vitro activation of [FeFe] hydrogenase: new insights into hydrogenase maturation. *J. Biol. Inorg. Chem.*, **2007,** *12*, 443-447.

(30) McGlynn, S. E.; Shepard, E. M.; Winslow, M. A.; Naumov, A. V.; Duschene, K. S.; Posewitz, M. C.; Broderick, W. E.; Broderick, J. B.; Peters, J. W.. HydF as a scaffold protein in [FeFe] hydrogenase H-cluster biosynthesis. *FEBS Lett.*, **2008,** *582*, 2183-2187.

(31) Drapal, N.; Maier, T. H. P.; Bock, A.. *Period Biol.*, **1998,** *100*, 45-51.

(32) Mulder, D. W.; Ortillo, D. O.; Gardenghi, D. J.; Naumov, A. V.; Ruebush, S. S.; Szilagyi, R. K.; Huynh, B. V.; Broderick, J. B.; Peters, J. W.. Activation of $HydA^{\Delta EFG}$ requires a preformed [4Fe-4S] cluster. *Biochemistry*, **2009,** *48,* 6240-6248.

(33) Jarrett, J.T.. The generation of 5'-deoxyadenosyl radicals by adenosylmethionine-dependent radical enzymes. *Curr. Opin. Chem. Biol.*, **2003,** *7*, 174-182.

(34) Nicolet, Y.; Rubach, J. K.; Posewitz, M. C.; Amara, P.; Mathevon, C.; Atta, M.; Fontecave, M.; Fontecilla-Camps, J. C.. X-ray structure of the [FeFe]-Hydrogenase Maturase HydE from *Thermotoga maritima. J. Biol. Chem.,* **2008,** *283*, 18861-18872.

(35) Ugulava, N.B.; Gibney, B.R.; Jarrett, J.T. Biotin Synthase Contains Two Distinct Iron-Sulfur Cluster Binding Sites: Chemical and Spectroelectrochemical Analysis of Iron-Sulfur Cluster Interconversions. *Biochemistry,* **2001,** *40,* 8343-8351.

(36) Taylor, A. M.; Farrar, C. E.; Jarrett, J. T., 9-Mercaptodethiobiotin Is Formed as a Competent Catalytic Intermediate by *Escherichia coli* Biotin Synthase. *Biochemistry,* **2008,** *47,* 9309-9317.

(37) King, P. W.; Posewitz, M. C.; Ghirardi, M. L.; Seibert, M.. Functional Studies of [FeFe] Hydrogenase Maturation in an Escherichia coli Biosynthetic System. *J. Bacteriol.*, **2006,** *188*, 2163-2172.

(38) Pilet, E.; Nicolet, Y.; Mathevon, C.; Douki, T.; Fontecilla-Camps, J. C.; Fontecave, M.. The role of the maturase HydG in [FeFe]-hydrogenase active site synthesis and assembly. *FEBS Lett.*, **2009,** *583*, 506-511.

(39) Peters, J. W.; Szilagyi, R. K.; Naumov, A.; Douglas, T.. A radical solution for the biosynthesis of the H-cluster of hydrogenase. *FEBS Lett.*, **2006,** *580,* 363-367.

(40) Brazzolotto, X., Rubach, J.K., Gaillard, J., Gambarelli, S., Atta, M., Fontecave, J.. The [Fe-Fe]-Hydrogenase Maturation Protein HydF from *Thermotoga maritima* Is a GTPase with an Iron-Sulfur Cluster. *J. Biol. Chem.*, **2006,** *2*, 769-774.

(41) Moncrief, M. C.; Hausinger, R. P.. Characterization of UreG, Identification of a UreD-UreF-UreG Complex, and Evidence suggesting that a Nucleotide-Binding Site in UreG Is Required for *In Vivo* Metallocenter Assembly of *Klbsiella aerogenes* Urease. *J. Bacteriol.*, **1997,** *179*, 4081-4086.

(42) Rangaraj, P.; Tyle, M. J.; Lanzilotta, W. N.; Ludden, P. W.; Shah, V. K.. *In Vitro* Biosynthesis of Iron-Molybdenum Cofactor and Maturation of the nef-encoded Apodinitrogenase. *J. Biol. Chem.*, **1999,** *274*, 19778-19784.

(43) Waldron, K. J.; Robinson, N. J.. How do bacterial cells ensure that metalloproteins get the correct metal?. *Nat. Rev. Microbi.*, **2009,** *6*, 25-35.

(44) Gasper, R.; Scrima, A.; Wittinghofer, A.. Structural Insights into HypB, a GTP-binding Protein That Regulates Metal Binding. *J. Biol. Chem.*, **2006,** *281*, 27492-27502.

(45) Scrima, A.; Wittinghofer, A.. Dimerisation-dependent GTPase reaction of MnmE: how potassium acts as GTPase-activating element. *EMBO J.*, **2006,** *25*, 2940-2951.

(46) Fish, W. W.. Rapid colorimetric micromethod for the quantitation of complexed iron in biological samples. *Methods Enzymol.*, **1988,** *158*, 357-364.

(47) Walker, J. E.; Saraste, M.; Runswick, M. J.; Gay, N. J.. Distantly related sequences in the alpha- and beta- subunits of ATP synthase, myosin, kinases and other ATP-requiring enzymes and a common nucleotide binding fold. *EMBO J.*, **1982,** *1*, 945-951.

(48) Pai, E. F.; Krengel, U.; Petsko, G. A.; Goody, R. S.; Kabsch, W.; Wittinghofer, A.. Refined crystal structure of the triphosphate conformation of H-ras p21 at 1.35 Å resolution: implications for the mechanism of GTP hydrolysis. *EMBO J.*, **1990,** *9*, 2351-2359.

(49) Paduch, M., Jelen, F., Otlewski, J.. Structure of small G proteins and their regulators. *Acta Biochim. Pol.*, **2001,** *48*, 829-850.

(50) Merzbacher, M.; Detsch, C.; Hillen, W.; Stulke, J.. *Mycoplasma pneumoniae* HPr kinase/phosphorylase signature sequence motif. *E. J. Biochem.*, **2004,** *271*, 367-374.

(51) Farnsworth, C. L.; Feig, L. A.. Dominant Inhibitory Mutations in the Mg^{2+}-Binding Site of RasH Prevent Its Activation by GTP. *Mol. Cell. Biol.*, **1991,** *11*, 4822-4829.

(52) Peters, J. W.; Lanzilotta, W. N.; Lemon, B. J.; Seefeldt, L. C. X-ray Crystal Structure of the Fe-Only Hydrogenase (CpI) from *Clostridium pasteurianum* to 1.8 Angstrom Resolution. *Science,* **1998,** 1853-1858.